10-15-1958

Semi-annual summary research report in metallurgy

Ames Laboratory Staff
Iowa State College

F. H. Spedding
Iowa State College

Semi-annual summary research report in metallurgy

Abstract
A semi-annual summary research report in metallurgy for the period of July through December 1957.

Metallurgy and Ceramics (UC-25)

U N C L A S S I F I E D

ISC-977

UNITED STATES ATOMIC ENERGY COMMISSION

RESEARCH AND DEVELOPMENT REPORT

SEMI-ANNUAL SUMMARY RESEARCH REPORT IN METALLURGY

For July - December, 1957

by

Ames Laboratory Staff

Date of Preparation
August 15, 1958

Date of Issuance
October 15, 1958

Ames Laboratory
at
Iowa State College
F. H. Spedding, Director
Contract W-7405 eng-82

U N C L A S S I F I E D

This report is distributed according to the category Metallurgy and Ceramics (UC-25) as listed in TID-4500, February 15, 1958.

Printed in USA. Price $2.50 . Available from the

Office of Technical Services
U. S. Department of Commerce
Washington 25, D. C.

ISC-977

TABLE OF CONTENTS

METALLURGY

SEMI-ANNUAL SUMMARY RESEARCH REPORT IN METALLURGY

For the period July - December, 1957

This report is prepared from material
submitted by the Group leaders
of the Laboratory

Previous research reports in this series are:

ISC-35
ISC-41
ISC-56
ISC-69
ISC-74
ISC-76
ISC-79
ISC-113
ISC-130
ISC-133
ISC-137
ISC-171
ISC-193
ISC-220
ISC-248
ISC-290
ISC-300
ISC-323
ISC-339
ISC-396
ISC-423
ISC-453
ISC-485
ISC-506
ISC-531
ISC-575
ISC-607
ISC-644
ISC-708
ISC-759
ISC-835
ISC-903

METALLURGY

Under the direction of F. H. Spedding, H. A. Wilhelm,
O. N. Carlson, P. Chiotti, R. E. McCarley,
D. T. Peterson and J. F. Smith.

1. Purification and Separation Studies

1.1 Studies on Liquid-Liquid Extraction (H. A. Wilhelm and M. L. Andrews)

Work of an exploratory nature has continued in this area with further use of thiocyanate in separation studies. Most of the work has been connected with zirconium-hafnium separation tests but other element-separation studies are being planned.

1.2 Separation of Particulate Impurities during Sublimation (D. T. Peterson and R. L. Skaggs)

The separation of thorium oxide and carbon from thorium tetrachloride had proven to be quite difficult by vacuum sublimation. Since these materials do not have an appreciable vapor pressure at the temperatures used in the sublimation of thorium tetrachloride, the failure to achieve a complete separation must result from the entrainment of particles of these impurities with the thorium tetrachloride vapor. The entrainment of a non-volatile particulate impurity in vacuum sublimation was studied by subliming ammonium chloride from mixtures containing silicon carbide.

The degree of purification obtained in a sublimation run was measured by determining the percentage of silicon carbide in the sublimed product. The results were expressed as a decontamination factor, which is the percentage of silicon carbide in the starting material divided by the percentage of silicon carbide in the product. The decontamination factor decreased with increasing sublimation rates and decreasing pressure on the system. A number of results are given in Table I. When the sublimation system was under dynamic vacuum,

Table I. Decontamination Factors in Vacuum Sublimation

Pressure	Temperature	Rate, g/hr	Decontamination Factor
Dynamic Vacuum	125°C	1.9	18
	150°C	54	15
	180°C	132	9
	210°C	216	1.9
3.5 mm	200°C	0.7	1000
	---	14	109
	235°C	79	25
	260°C	165	20
	280°C	316	4
11.0 mm	230°C	18	292
	245°C	44	120
	270°C	122	65
	275°C	222	23
43.5 mm	250°C	7	1000
	255°C	36	228
	270°C	87	121
	290°C	215	71

the decontamination factor was rather low even at extremely low rates. Sublimation with a constant pressure maintained on the system gave much better decontamination factors. In some cases the amount of silicon carbide was too small to be weighed and was detected only by a slight tint of gray on the filter paper.

The particle sizes of the original silicon carbide and of silicon carbide entrained during sublimation were determined. Since small particles can be carried by a gas stream at lower velocities than large particles, entrained silicon carbide was expected to have a smaller fraction of large particles. This was confirmed by the results given in Table II. Particles

Table II. Particle Size Distribution of Silicon Carbide

Particle Diameter, microns	Cumulative Weight Percent		
	Original	Poor Separation	Good Separation
< 24	75	100	100
< 20	58	88	100
< 16	30	74	93
< 12	17	42	54
< 8	6	12	30

greater than 24 microns in diameter were absent in the entrained silicon carbide although these particles constituted 25 percent of the original sample. The particles entrained in a sublimation run which resulted in a poor separation (decontamination factor of 15) were coarser than those from a run resulting in a decontamination factor of 106. The small particles which are entrained would be more difficult to separate in a second sublimation and lower decontamination factors would be expected for resublimation.

1.3 Precipitation of Thorium Hydride from Thorium Magnesium Solution (P. Chiotti and P. F. Woerner)

A report (ISC-928) entitled "Precipitation of Thorium Hydride from Thorium Magnesium Solutions" by Paul F. Woerner and P. Chiotti is being distributed.

Abstract

The precipitation of thorium as thorium dihydride from thorium-magnesium solutions has been investigated over the temperature range of 665° to 810°C at one atmosphere hydrogen pressure. The concentration of thorium in the liquid phase for the reactions carried out at one atmosphere hydrogen pressure over the specified temperature range is given by the following relation:

$$\log_{10} N_{Th} = \frac{-4609 \pm 209}{T} + 2.824 \pm 0.208,$$

where N_{Th} represents the mole fraction of thorium in the liquid phase.

Analytical expressions have also been determined, whereby the activity coefficient of thorium in the liquid solutions relative to liquid or relative to solid thorium at the equilibrium concentrations for a given temperature, can be calculated.

2. Preparation of Pure Compounds

2.1 Preparation of Pure Vanadium Pentoxide (R. E. McCarley and J. W. Roddy)

Three methods for the preparation of high purity V_2O_5, which can be used for the preparation of high purity vanadium metal, have been studied and are described below. The starting material in each case was an impure oxide (ca 85% V_2O_5) which was recovered from the processing of uranium ores.

(1) Since the reaction of ethanol with V_2O_5 is known to produce ethyl orthovanadate, a volatile liquid, it seemed worthwhile to investigate the reaction as a possible means of purifying V_2O_5. The proposed scheme was to form ethyl orthovanadate by the reaction

$$V_2O_5 + 6C_2H_5OH \rightleftharpoons 2VO(OC_2H_5)_3 + 3H_2O,$$

free it of impurities by distillation and subsequently

hydrolyze to recover V_2O_5. Under the various conditions investigated, little or no $VO(OC_2H_5)_3$ was formed and the method was dropped as being impractical.

(2) A method which is in common use for the production of cp V_2O_5 involves dissolution of the impure material in sodium carbonate solution, filtration to remove insoluble metal hydroxides, precipitation of NH_4VO_3 with ammonium chloride and subsequent ignition to V_2O_5. Using this method we have found that several elements, notably Si, Cr, Mg, Al and Cu were not removed satisfactorily from the vanadium. However, the addition of ca 1000 ppm of either citric or tartaric acid to the carbonate solution before precipitation of the NH_4VO_3 greatly reduced the concentration of these impurities in the product.

(3) The chlorination of the impure oxide proved to be the most effective method for removing impurities and compared very favorably in cost with method (2). The principal features of this process are the following: (a) a mixture of the oxide and carbon were chlorinated at 300-400°C to produce the volatile $VOCl_3$, which distilled out of the reaction chamber and was condensed, (b) the $VOCl_3$, bp 127°C, was distilled, (c) hydrolysis of the $VOCl_3$ was performed in 3-4N ammonia solution to precipitate NH_4VO_3 and (d) the NH_4VO_3 was ignited at 500-600°C to produce high purity V_2O_5. A typical

analysis of this oxide showed purity in excess of 99.95% V_2O_5 with only trace amounts of Si, Cr, Mg, Al and ca 20 ppm N_2. There was evidence that deviations from the formula V_2O_5 occurred in some cases because of partial reduction of the vanadium to lower oxidation states during hydrolysis of the $VOCl_3$. Preliminary results of chlorinations carried out in an all-glass, rotating tube reactor designed to produce pound lots of V_2O_5 indicate both high chlorine conversion efficiency and good vanadium recovery.

2.2 Preparation of Pure Metal Carbonyls (R. E. McCarley and B. W. Farnum)

Many of the transition metals can be prepared in a high state of purity by thermal decomposition of their volatile, metal carbonyl compounds. At the present time the application of this technique is restricted to the metals of groups VIb, VIIb and VIIIb, since the carbonyls of the remaining transition metals have not been prepared. Recently, however, evidence has appeared which indicates that the carbonyls of the groups IVb and Vb metals can, indeed, be prepared by the application of modern high pressure techniques, and the utilization of formerly unknown or unavailable starting materials. A research program has been initiated to encompass the following objectives: (a) to improve existing methods of synthesis and

devise new methods which may result in preparation of unknown carbonyls, (b) to study the decomposition reactions of metal carbonyls with a view towards preparation of high purity metals and (c) to undertake some structural investigations which may improve our understanding of the bonding in metal carbonyl compounds. Work during this period has been limited to obtaining the necessary high pressure apparatus and synthesis of some necessary starting materials. Initial efforts will be directed toward preparation of vanadium and niobium compounds containing metal-to-CO bonds.

2.3 Preparation of Yttrium Fluoride (O. N. Carlson, F. A. Schmidt, and F. H. Spedding)

A considerable quantity of yttrium trifluoride was prepared during this period by the direct hydrofluorination of high purity Y_2O_3. This fluoride was employed in the preparation of yttrium metal as is described in a later section of this report. The conditions under which the reaction was carried out were as follows. The Y_2O_3 was placed in an inconel tube which was inserted in an electrically heated resistance furnace. Anhydrous HF was passed over the oxide as the furnace temperature was raised to 700°-750°C over a period of 5 to 6 hours. An HF flow was maintained over the material at this temperature for an additional three hours

with periodic rotation of the tube and its contents. Chemical and spectrographic analysis of the fluoride thus produced indicated that conversions of greater than 99.5% were obtained. The oxygen content of the material was estimated at less than 0.1 w/o O_2.

In an attempt to prepare a higher quality fluoride than that described above, a series of dual cycle hydrofluorination experiments was undertaken. The first eight-hour cycle was run at a low temperature and the second or "topping" cycle was run at 750°C for 3 hours. The low temperature cycle was run at temperatures of 200, 300, 400 and 500°C in the separate experiments. The quality of the fluoride produced under each set of conditions was ascertained by the spectrographic method which gives the relative oxygen content. While no large differences were observed, the fluoride prepared at the higher initial furnace temperature appeared to contain lesser amounts of unconverted oxide or oxyfluoride. The quality of the fluoride was somewhat improved by applying some of the principles learned from these tests, such as knowledge of the criticality of HF gas flow and adequate exhaust facilities. Extimates place the oxygen content of the fluoride prepared under these more carefully controlled conditions below 0.05 w/o O_2.

3. Metal Preparation Studies

3.1 Preparation of Vanadium Metal

3.1.1 By the Iodide Process (O. N. Carlson and C. V. Owen)

During this period approximately 5 lbs of crystal bar vanadium metal were prepared for use in the research programs described in later sections of this report. Most of this material was prepared in a newly constructed inconel retort which yielded about one-half pound of vanadium metal per batch. This metal was prepared by using the following conditions, which were found to be optimum for an apparatus of the design employed. The filament temperature was maintained at 1050° to 1150°C, the feed material at 800° to 825°C and the initial vacuum on the system was 2×10^{-5} microns.

The purity of the crystal bar prepared to date is estimated to be 99.9+% vanadium with trace amounts of Ca, Cr, Cu, Fe, Mg, Si and Ti. Most of these metallic impurities are carried over from the feed material. The interstitial impurities, carbon, oxygen and nitrogen, are present in a total amount estimated to be less than 400 ppm. Analytical procedures for determining oxygen and nitrogen somewhat more accurately are presently being developed. Arc-melted specimens of this material had Rockwell E hardness values

from 50 to 75 and could be cold rolled extensively without evidence of cracking. Twenty-five mil wire has been prepared by cold swaging. No intermediate annealing steps were required in these operations.

3.1.2 By Reductions of V_2O_5 (H. A. Wilhelm and K. M. Wolf)

Variations of the carbon-to-V_2O_5 ratio in the charge for preparing vanadium metal indicate that less than five (5) carbons to one (1) vanadium pentoxide is stoichiometric for the reaction carried out in a vacuum at elevated temperatures. At a temperature of 1550°C and in a vacuum, most of the charge is reacted to give a sponge metal containing both oxygen and carbon. The reaction fails to go to completion and the resulting metal after arc-melting is hard and brittle. It is possible that heating the sponge in a vacuum to a higher temperature than 1550°C could reduce the residual oxygen and carbon in the vanadium. A container for vanadium metal, especially when the metal is molten, is a problem in this phase of the work. A UO_2 crucible has been employed here and the resulting metal after arc melting was not as hard as obtained when the charge was heated to only 1550°C in graphite before arc melting.

3.2 Preparation of Niobium Metal

3.2.1 By Carbon Reduction of Cb_2O_5 (H. A. Wilhelm and E. R. Stevens)

Further tests on TiO_2 and SiO_2 as additives in the reduction of Cb_2O_5 with carbon are being made. In making up a charge of Cb_2O_5 and carbon it has been found essential to precalcine the Cb_2O_5 to reduce the amount of volatiles. The slight variation in Cb_2O_5 to carbon ratio caused by volatiles in either constituent can give ratios far from those planned and result in excess oxygen or excess carbon. One commercial pentoxide of columbium contained as much as 8.85% volatiles. In studying the effects of additives, the Cb_2O_5 to carbon ratio has to be known and reproducible. The mechanism resulting in the beneficial effect of TiO_2 additions to the charge has not been fully worked out as yet. Some work on the TiO_2-carbon reaction is planned in connection with the interpretation of the effect of the TiO_2 additions.

3.2.2 By Reduction of Nb_2O_5 with Ca, Mg, and Al (H. A. Wilhelm and T. G. Ellis)

The reaction of Ca with Nb_2O_5 was investigated. This reaction was predicted to be

$$5Ca + Nb_2O_5 \rightleftharpoons 5CaO + 2Nb.$$

Reactions were run in a 1 1/2-inch diameter steel bomb with a 1-inch diameter reaction chamber lined with electrically fused dolomitic oxide. The amount of Ca was varied from stiochiometric to 50% excess. In each case no metal button was found, but metal was found microscopically divided in the slag phase. This metal in the slag phase was not readily reclaimable. The external temperature of the bomb was approximately 780°C at the firing point and this temperature rose an additional 35°C maximum after firing.

In each case the slag from the Ca reduction was black in color giving evidence of a lower form of niobium oxide, probably NbO or NbO_2. Since this oxide is quite soluble in Nb metal, this method of reducing Nb_2O_5 was temporarily abandoned.

Several reactions of Nb_2O_5 with a Ca-Mg alloy were run to determine the firing temperature metal purity and yield. The alloy consisted of 66 a/o Ca and 34 a/o Mg. The reaction was predicted to be

$$Nb_2O_5 = 5(.66Ca+.34Mg) \rightleftharpoons 2Nb + 5(.66CaO+.34MgO).$$

The reactions were run with stoichiometric amounts of reactants in the 1 1/2-inch bomb as described above for calcium reduction. The firing temperature was approximately 790°C. A finely divided metal phase was found dispersed in

the slag. This metal was qualitatively analysed spectroscopically and showed very little contamination with Ca or Mg. In all reactions the slag phase was blue in color, indicating the presence of Nb_2O_3, a product of incomplete reduction.

Another reaction was run using a liner of CaO and only metallic Ca as a reductant. No massive metal was found after reaction. The slag was black in color indicating the presence of NbO, a product of an incomplete reduction.

Inasmuch as some form of niobium oxide was present in each reaction product regardless of conditions of reaction, the Ca-Mg reduction method does not appear to be feasible.

The reaction of Nb_2O_5 with Al was predicted to be:

$$3Nb_2O_5 + 10Al \rightleftharpoons 6Nb + 5Al_2O_3$$

This reaction was similarly run in the 1 1/2-inch steel bomb. The amount of Al was varied from stoichiometric to 10% excess. The average firing temperature of the reaction was 900°C and the average maximum temperature was 1000°C. Each reaction produced massive metal. Slag-metal separation in each reaction was excellent. The metal produced in reactions with less than 2% excess Al was solid while greater than 2% excess Al produced porous metal. The slag was difficult to remove from the surface of the metal. The

metal obtained with less than 2% excess Al reactant was hard and tough while that from greater than 2% excess was hard and brittle. Precise information as to the chemical composition of the alloy product is not available at this time.

In order to further study slag adherence to the metal, small additions of MnO_2 were made to stoichiometric and 2% excess Al in the reaction

$$3Nb_2O_5 + 10Al \rightleftharpoons 6Nb + 5Al_2O_3.$$

These reactions were run as before. The firing temperature of the stoichiometric Al reaction and 2% excess Al reaction was approximately 925°C. No significant difference in firing temperature was noted for the various amounts of MnO_2. However the slag adherence to the metallic phase differed greatly. For stoichiometric Al and low MnO_2, there was very little slag adherence and the slag was crystalline. For the 2% excess of Al and high MnO_2, the slag was amorphous and adhered to the metal. In all cases the slag-metal segregation was very good.

The reduction of Nb_2O_5 with Al will be investigated further. This investigation will consist of studying methods of removing the Al from the Nb-Al alloy produced in the reaction mentioned above. An attempt will also be made to construct the phase diagram for the Nb-Al alloy system.

3.2.3 By the Iodide Process (R. E. McCarley and W. Tadlock)

The purpose of this investigation was to study the preparation of high purity niobium metal by the iodide process and to provide a supply of this metal within the laboratory for experimental purposes. A power supply and vacuum system for the process has been constructed for use with a glass iodide cell. Filament temperature during operation of the cell will be controlled with the aid of the relation

$$EI^{1/3} = K = L(4\pi\rho\, a^2\sigma^2T^8)^{1/3} = K'L$$

where E = voltage

I = current in amperes

K = constant which is a function of filament temperature and length

a = emissivity

σ = 5.735×10^{-12} w/cm^2-°K for a black body

T = temperature in degrees Kelvin

ρ = resistivity

$$K' = (4\pi\rho\, a^2\sigma^2T^8)^{1/3} = \frac{EI^{1/3}}{L} .$$

The constant K' is independent of the filament diameter and thus may be used for regulation of current and voltage to maintain the desired temperature. With this in mind, K' has

been determined as a function of temperature in the range 800 to 1400°C for niobium wires of 0.010 in. and 0.025 in. diameter. Agreement of the K' values for the two wires was excellent. Temperatures were measured with a Leeds and Northrup optical pyrometer and appropriate corrections were made for emissivity of the niobium wire and absorption by the sight glass. The apparatus consisted of an evacuated pyrex tube fitted with tungsten electrodes for suspension of the filament, a variable ac power supply, and a voltmeter and ammeter for measurement of the filament current and voltage.

3.3 Preparation of Thorium

3.3.1 By the Iodide Process (D. E. Williams, O. D. McMasters and P. E. Palmer)

The pyrex-glass apparatus for producing iodide thorium is now working satisfactorily and yields of about 200 g per run are being obtained. Trials with a metal reaction vessel in which the thorium was deposited on a metal hot-finger have not been successful to date. The deposited thorium was found to react with Inconel at the deposition temperature and other less active metals are to be tested.

3.3.2 By the Ca-Mg Reduction of ThF_4 (H. A. Wilhelm, R. L. Snyder and E. P. Neubauer)

Studies of the reduction of thorium compounds with calcium

and magnesium metals are planned on the basis of certain reported phase diagram relationships. It is known that the melting point of thorium, which is about 1750°C, is lowered considerably by the addition of magnesium metal. It is also known that calcium fluoride and magnesium fluoride form a eutectic mixture. The objective of this investigation is to develop conditions so that a charge of ThF_4, calcium and magnesium can form products of the low-melting Th-Mg alloy and the low-melting CaF_2-MgF_2 slag from which the metal phase can be recovered and subsequently treated to give a good yield of good quality thorium metal. Most of the work in this area has so far been directed toward testing of the phase relationships and testing the reactions of mixtures of calcium and magnesium and of calcium-magnesium alloys with UF_4 as a stand-in for ThF_4. Good biscuit uranium metal was obtained as expected and the slag phase developed as predicted. Work has only been initiated on the reaction of primary interest and results thus far look promising for the preparation of thorium by this reduction.

3.4 Preparation of Yttrium Metal (O. N. Carlson, D. T. Eash, J. Haefling, F. A. Schmidt and F. H. Spedding)

Studies on the preparation of yttrium metal by the reduction of YF_3 with calcium in the presence of magnesium metal and $CaCl_2$ have continued. The reductions were carried

out under an inert atmosphere in a zirconium vessel which was placed in a mild steel retort and heated in a gas-fired furnace to temperatures of 950 - 975°C.

A low melting, brittle Y-25 w/o Mg alloy was obtained as the reduction product. The magnesium was subsequently removed by heating crushed pieces of the alloy under vacuum to 1200°C. The alloy was contained in a titanium vessel during this operation. The resulting sponge was compacted into bars for use as electrodes in a consummable arc-melter. A second arc-melting step carried out under vacuum resulted in solid castings free of residual voltile impurities such as calcium and magnesium.

The reduction operation was scaled up successfully to produce approximately 130 lbs of alloy in a single reduction. The magnesium removal operation was likewise scaled up to handle this quantity of alloy. It was found that a double heating operation involving approximately 16 hours of total heating time was required to remove the calcium and magnesium sufficiently to permit satisfactory arc melting of the sponge. Ingots 6 in. in diameter by 19 in. in height and weighing 85 lbs have been successfully arc melted by the double melting procedure. A typical chemical analysis of yttrium metal prepared in this way is given in Table III.

Table III. Chemical Analysis of a Representative Yttrium Ingot

Element	w/o
Carbon	0.020
Nitrogen	0.010
Iron	0.015
Titanium	0.006
Zirconium	0.5 - 1.0
Calcium	< 0.001
Magnesium	< 0.003
Copper	< 0.005
Silicon	< 0.020
Boron	< 0.001
Nickel	0.030
Oxygen	0.2 - 0.4

In addition to the large scale experiments, a number of small reductions were carried out which were designed primarily to improve the purity of the metal, particularly with regard to the oxygen content. In one series of experiments, YF_3 was reduced by lithium metal to form an Y-Mg alloy under conditions very similar to those employed with calcium. This made possible the elimination of calcium and calcium

chloride. Both of these chemicals are potential contributors of oxygen to the yttrium metal. In the first experiment the lithium metal was used as-received with only a surface cleaning treatment. The yttrium metal that was obtained contained 0.37 w/o oxygen and 0.09 w/o nitrogen. In a second experiment the lithium was filtered prior to use in the reduction, and in duplicate experiments yttrium containing 0.16 w/o and 0.24 w/o oxygen was obtained. The nitrogen content was also lower (0.02 w/o).

Another series of experiments included the addition of various types of oxides to the reduction charge to ascertain which ones transfer their oxygen to the yttrium during the reduction step. Calcium oxide, yttrium oxide, and yttrium oxyfluoride were each mixed intimately with the charge in the reduction step. In each case the oxygen was quantitatively transferred to the yttrium metal as indicated by the oxygen analyses of the metal. From these experiments it was concluded that any oxygen-containing compound in any of the ingredients would probably introduce oxygen into yttrium metal during this processing step.

Assuming that granular calcium and magnesium contain significant amounts of surface oxides, experiments were performed in which freshly redistilled chunk-calcium was

employed as the reductant. For comparison, similar reductions were performed in which the calcium reductant was in the form of granular particles approximately 1/8 in. in diameter. This too had been freshly redistilled prior to grinding. The results of this comparison are presented in Table IV.

Table IV. Effect of Particle Size of Calcium Reductant on Oxygen Content of Yttrium Metal

Experiment	w/o O_2 in Y metal
Granular calcium	0.33
Granular calcium	0.32
Massive calcium	0.24
Massive calcium	0.22

These experiment show rather conclusively that grinding of the calcium results in an increased oxygen content of yttrium metal and that an improved metal product can be obtained by using massive calcium and magnesium.

Attempts were made to purify yttrium metal by vacuum distillation from a tantalum crucible. Vapor pressure data indicated that yttrium can be vacuum distilled at a temperature

of 1900°C. Approximately 50 g of redistilled yttrium were collected on a tantalum condensor and chemically analyzed for comparison with the purity of the initial metal. The results are given in Table V.

Table V. Results of Yttrium Metal Distillation Experiments

Impurity	Amount Present Before Distillation	After Distillation
C	150 ppm	50 ppm
N	95 "	95 "
O	1975 "	2000 "
Fe	400 "	175 "
Zr	7000 "	not detected
Ca	500 "	trace
Mg	300 "	500 ppm
Si	500 "	very weak
Cu	trace	very weak
Br_2 insoluble	0.59%	0.58%

3.5 Preparation of Uranium Metal (H. A. Wilhelm, E. P. Neubauer and R. L. Snyder)

One of the older processes for making uranium metal is being reinvestigated. This is the carbon reduction of uranium oxide which was reported by Moissan many years ago. His product usually contained intolerable amounts of carbon. Early in 1942 a quick experimental look at this process at Ames produced similar results. Sylvania in recent years has done work on this reaction but satisfactory metal in low yields has been obtained only by employing certain treatments subsequent to reduction.

The objective of the current work is to obtain satisfactory quality uranium metal directly on the reduction step. The reaction between uranium dioxide and carbon requires a high temperature at reduced pressure. The container for such a charge then becomes a problem. When a charge is heated in a graphite crucible to about 2200°C to complete the reaction, there is considerable attack on the crucible. Graphite crucibles lined with UO_2 gave indication of better results; however, there was some reaction between the graphite and its liner. A barrier coating of ZrO_2 on the graphite gave results that appeared promising but is not the entire solution. The temperature employed at present is sufficient to cause volatilization of UO_2 liner material.

3.6 Preparation of Tantalum Metal (H. A. Wilhelm and C. B. Hamilton)

A number of methods have been employed to produce tantalum metal. The carbon reduction of tantalum pentoxide is to be investigated to determine the carbon to oxide ratio and the temperature necessary for carrying out the reaction under vacuum conditions. Other methods for preparing the metal will also be studied.

4. Alloy Systems

4.1 Solubility of Uranium in Zinc and Thermodynamic Properties of U_2Zn_{17} (P. Chiotti and H. Shoemaker)

The solubility of uranium in liquid zinc has been determined using the same apparatus and experimental procedure used in studying the solubility of uranium in magnesium and magnesium-thorium solutions. The results obtained are given in Table VI. These values are in good agreement with those determined by Knighton in U. S. Atomic Energy Commission Report ANL 5753.

Vapor pressure data from an earlier investigation of the uranium-zinc system [see ISC-656 or P. Chiotti, H. H. Klepfer, and K. J. Gill, Uranium-Zinc System, J. Metals, 9, 51-57 (1957)] were utilized in calculating the free energy of formation of U_2Zn_{17}. A least squares treatment

of the vapor pressure data for 35 and 65 w/o uranium-zinc alloys gave

$$\log_{10} P_{Atm} = -\frac{7.713 \pm 60}{T} + 6.33 \pm 0.06. \qquad (1)$$

This equation represents the zinc vapor pressure over a temperature range of 650 to 940°C in the two-phase, U-U_2Zn_{17} region of the equilibrium diagram.

Table VI. Solubility of Uranium in Zinc

No. of Samples Taken at 1 hr intervals	Temperature °C	Average w/o Uranium	Average a/o Uranium
3	475	0.005	0.0014
3	550	0.083	0.023
1	625	0.38	0.10
2	700	1.06	0.29
3	800	4.83	1.58

The compound reported to be UZn_9 has been shown by Makarov and Vinogradov to correspond more closely to the formula U_2Zn_{17} [E. S. Makarov and S. I. Vinogradov, Crystal Structure of Th_2Zn_{17} and U_2Zn_{17}, Kristallografiia 1, 634-643, (1956)]. Unpublished work by D. Peterson and C. Vold also indicates that this is the correct formula and that the

crystal structure is similar to that for the compounds Th_2M_{17} investigated by Florio, et al.; here M represents iron, cobalt or nickel. [J. V. Florio, N. C. Baenziger, and R. E. Rundle, Compounds of Thorium with Transition Metals. II. Systems with Iron, Cobalt, and Nickel, Acta Crystallographica 9, 367-372, (1956).]

Kelley [K. K. Kelley, Contributions to the Data of Theoretical Metallurgy No. III, The Free Energies of Vaporization and Vapor Pressure of Inorganic Substances, U. S. Dept. of the Interior, Bur. of Mines Bulletin 383, (1935)] gives the following relations for the free energy of vaporization of liquid and solid zinc.

$$\Delta F^o = 30,902 + 6.03T \log T + 0.275 \times 10^{-3}T^2 - 45.03T \qquad (2)$$

and

$$\Delta F^o = 31,392 + 0.64T \log T + 1.35 \times 10^{-3}T^2 - 31.17T, \qquad (3)$$

respectively. With equation (1) for the vapor pressure of zinc over the alloy we obtain

$$\Delta F = -RT\ln K = -2.303RT - \frac{7.713 \pm 60}{T} + 6.33 \pm 0.06$$
$$= 35,287 \pm 275 - 28.96 \pm 0.275T. \qquad (4)$$

Consequently for the reaction

$$2U\,(S) + 17Zn(\ell) \longrightarrow U_2Zn_{17}\,(S),$$

$$\Delta F^o = 17\,[-4,385 \pm 275 + 6.03\,T \log T + 0.275 \times 10^{-3}T^2 - 16.07 \pm 0.275T]. \qquad (5)$$

Similarly for the reaction

$$2U\ (S) + 17\ Zn(S) \longrightarrow U_2Zn_{17}\ (S),$$

we obtain

$$\Delta F^{\circ} = 17\ \angle -3{,}895 \pm 275 + 0.64T \log T + 1.35 \times 10^{-3}T^2 - 2.21 \pm 0.275T\ \_/. \qquad (6)$$

The standard enthalpy and entropy change can then be calculated from the relations

$$\frac{\delta \Delta F^{\circ}/T}{\delta\ 1/T} = \Delta H^{\circ} \text{ and } \frac{\delta \Delta F^{\circ}}{\delta\ T} = -\Delta S^{\circ}.$$

Equation (6) was used to calculate the values given in Table VII for a temperature of 25°C, while equation (5) was used to calculate the other values given. The calculations at 25°C represent a rather large extrapolation of the vapor pressure curve. The calculations of the probable errors do not include any error inherent in K. K. Kelley's equations for the free energy of vaporization or sublimation of pure zinc.

Table VII. Thermodynamic Properties of U_2Zn_{17}

Temperature °K	Temperature °C	$-\Delta F^{\circ}$ Kcal/mole	$-\Delta H^{\circ}$ Kcal/mole	$-\Delta S^{\circ}$ cal/°C mole	Probable Error ΔF°	Probable Error ΔH°	Probable Error ΔS°
298	25	67.4	69.7	7.6	5.3	4.7	4.7
773	500	54.0	111.8	74.6	5.9	4.7	4.7
1073	800	28.9	127.6	92.0	6.8	4.7	4.7

4.2 Thorium-Yttrium System (O. N. Carlson and D. T. Eash)

A series of yttrium-thorium alloys at approximately 10 w/o composition intervals were prepared by arc melting together yttrium sponge and crystal-bar thorium. The melting points of these alloys were determined by an optical pyrometer method from which the solidus has been tentatively determined to be a continuous curve extending from the melting point of yttrium to that of thorium. While these data indicate extensive or complete solid solubility at high temperatures, this has not been confirmed by microscopic evidence. Difficulty has been encountered in polishing and etching the alloys of this system.

4.3 Tantalum-Zirconium System (D. E. Williams and P. J. Jackson)

The termination of the eutectoid horizontal on the tantalum-rich side of the diagram has been established by temperature-resistance and X-ray data. This had previously been reported as 94% tantalum, but on the basis of recent work, 96 ± 1% tantalum seems a better value. The solubility of zirconium in tantalum at room temperature was determined as 2% by X-ray diffraction methods. This and other X-ray work, and also the temperature-resistance data, have established the path of the solvus on the tantalum-rich side.

An extensive metallographic study is still being conducted on the tantalum-zirconium system in the range from 0.5 to 20% tantalum. This is being done in an effort to determine the eutectoid composition. Results of this study place the eutectoid at about 10% tantalum. The metallographic experiments have also fixed the solubility limit of tantalum in alpha zirconium between 1.5 and 2.0%.

4.4 Zinc-Zirconium System (P. Chiotti and G. Kilp)

The phase boundaries of the zinc-zirconium system were determined in previous work. The phase diagram as determined under constrained vapor conditions, zinc vapor pressure-temperature relations for a number of these alloys, and a summary of information on the five intermetallic compounds found in this system has been previously reported (ISC-837). The phase diagram at one atmosphere pressure is given in Fig. 1.

4.4.1 Thermodynamic Properties

Equations for ΔH_f°, ΔF_f°, and ΔS_f° for the five compounds over a range of temperatures have been derived from the vapor pressure data. Table VIII gives the analytical expressions for the zinc vapor pressure used in these calculations. Table IX contains calculated values of these quantities at 25, 500, 750, and 900°C (298, 773, 1023, and 1173°K). The procedure

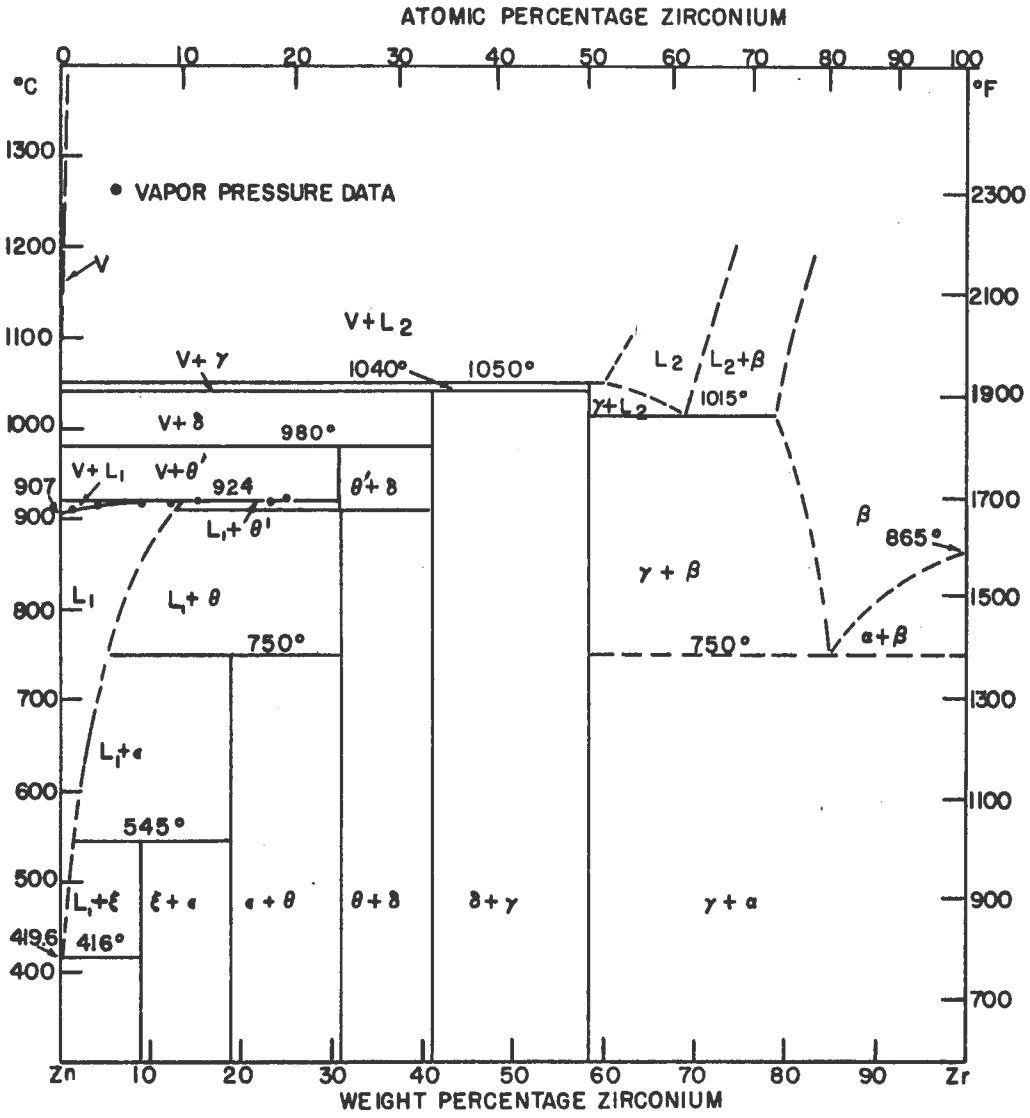

Fig. 1 - Zinc-zirconium phase diagram at one atmosphere pressure.

employed in calculating these quantities was essentially the same as that outlined for the calculation of the thermodynamic properties for U_2Zn_{17} outlined above.

Table VIII. Zinc vapor pressure as a function of temperature for five of the two phase regions of the zinc-zirconium system

$$\log_{10} P^* = AT^{-1} + B$$

Equilibrium Phases	A	B	Temperature Range °K
Zr + ZrZn	-12,918 ± 125	9.603 ± 0.119	800 - 1180
ZrZn + $ZrZn_2$	- 8,440 ± 110	6.401 ± 0.099	940 - 1225
$ZrZn_2$ + $ZrZn_3$	- 8,792 ± 80	7.053 ± 0.076	900 - 1200
$ZrZn_3$ + $ZrZn_6$	- 7,448 ± 87	6.488 ± 0.095	850 - 1200
$ZrZn_6$ + $ZrZn_{14}$	- 7,171 ± 82	6.441 ± 0.104	750 - 820

* The pressure P is in atmospheres, and the temperature T is in degrees Kelvin. Values for the constants A and B are given in the table along with their probable error as determined from a least squares treatment of the data.

4.4.2 Eutectic Composition

Additional thermal analyses and microscopic examinations of alloys of near eutectic composition were made in an attempt

Table IX. Calculated values for ΔF_f°, ΔH_f°, and ΔS_f° at 25, 500, 750, and 900°C

Compound	Temp. (°K)	$-\Delta F_f^\circ$ Kcal/mole	$-\Delta H_f^\circ$ Kcal/mole	$-\Delta S_f^\circ$ Cal/deg-mole	Prob. Error ΔF_f° Kcal/mole	Prob. Error ΔH_f° Kcal/mole	Prob. Error ΔS_f° cal/mole °K
ZrZn	298	23.3	27.9	15.5	± 0.6	± .6	± 0.5
$ZrZn_2$	298	30.5	35.3	16.2	± 1.1	± 1.1	± 1.0
$ZrZn_3$	298	37.7	44.4	22.5	± 1.5	± 1.4	± 1.3
$ZrZn_6$	298	44.7	53.0	28.0	± 2.6	± 2.6	± 2.6
$ZrZn_{14}$	298	55.3	66.0	35.7	± 5.8	± 5.6	± 5.6
ZrZn	773	15.4	30.4	19.4	± 0.7	± .6	± 0.5
$ZrZn_2$	773	21.7	40.3	24.1	± 1.3	± 1.1	± 1.0
$ZrZn_3$	773	25.6	51.8	33.8	± 1.8	± 1.4	± 1.3
$ZrZn_6$	773	29.8	67.9	49.2	± 3.3	± 2.6	± 2.6
$ZrZn_{14}$	773	32.3	100.7	88.4	± 7.1	± 5.6	± 5.6
ZrZn	1023	10.5	31.1	20.2	± 0.8	± .6	± 0.5
$ZrZn_2$	1023	15.4	41.8	25.8	± 1.5	± 1.1	± 1.0
$ZrZn_3$	1023	17.0	54.1	36.4	± 2.0	± 1.4	± 1.3
$ZrZn_6$	1023	17.0	72.6	54.4	± 3.8	± 2.6	± 2.6
ZrZn	1173	7.4	31.6	20.7	± 1.2	± .6	± 0.5
$ZrZn_2$	1173	10.7	42.8	26.7	± 1.6	± 1.1	± 1.0
$ZrZn_3$	1173	9.9	55.6	37.8	± 2.2	± 1.4	± 1.4

to establish more precisely the eutectic composition and temperature. The thermal analyses were not particularly helpful in establishing the eutectic composition. However, examination of the microstructure of alloys containing 0.1, 0.2, 0.3, 0.4, 0.5, and 0.9 w/o zirconium indicated that the eutectic composition is close to 0.3 w/o zirconium. None of these alloys appear to be 100% eutectic structure. Compositions greater than 0.3 w/o zirconium contained relatively large primary $ZrZn_{14}$ crystallites and in some areas relatively large zinc crystals in addition to typically finely dispersed eutectic structure. The larger zinc grains in these alloys were presumably formed by agglomeration of the finely dispersed zinc crystallites of the eutectic during solidification. Alloys containing 0.3 w/o or less zirconium contained relatively large primary zinc dendrites with little or no evidence of large $ZrZn_{14}$ crystallites which could be interpreted as a primary phase. The best value for the eutectic composition is therefore taken to be 0.3 ± 0.05 w/o zirconium, or $N_{Zr} = 0.002 \pm 0.0004$.

The best value for the eutectic temperature obtained by the thermal analyses was $417 \pm 1.0°C$. Assuming that the dilute solutions formed behave ideally, the melting point lowering of zinc at a composition of 0.2 a/o zirconium would be roughly 1.0°C. Conversely, accepting the eutectic temperature to be 417°C, which corresponds to a melting point lowering of

2.5°C, the calculated composition is 0.5 a/o zirconium. The microstructures indicate that this value is too high.

4.4.3 Liquidus Curve for Zinc-Rich Alloys

The solubility of zirconium in zinc as estimated from zinc vapor pressure lowering data, thermal data and other observations made in the course of the study of this system is given in Table X. These data are to be considered tentative and an attempt will be made to obtain more precise values by direct measurements.

Table X. Estimated Solubility Range of Zirconium in Zinc

Temperature °C	Atomic Fraction N_{Zr}	w/o Zr
417	0.0018 - 0.0025	0.25 - 0.35
500	0.0054 - 0.0080	0.75 - 1.12
600	0.013 - 0.020	1.81 - 2.8
700	0.028 - 0.043	3.92 - 6.0
800	0.050 - 0.070	7.0 - 9.8
900	0.084 - 0.102	11.7 - 14.2
1000	0.105 - 0.120	14.7 - 16.8

4.5 Tantalum-Vanadium System (O. N. Carlson and D. T. Eash)

The investigation of the intermediate phase in the tantalum-vanadium system has continued during this period. A powder pattern of this compound was tentatively indexed on the basis of a hexagonal lattice with a = 5.065A and c = 11.703A. The structure of this compound was not determined, however, and additional work will be required for an unambiguous determination. An alloy of a composition lying close to TaV_2 was homogenized at 1700°C and then annealed at 1200°C for 120 hours. Microscopic examination of the heat-treated alloy indicated that the composition of the intermediate phase lies at or near the TaV_2 composition.

4.6 Thorium-Hydrogen System (D. T. Peterson and D. G. Westlake)

The solubility of thorium hydride in thorium was determined from 300° to 800°C. The solubility as a function of temperature for thorium metal with different impurity levels is shown in Fig. 2. The logarithm of the solubility in atomic percent is plotted against the reciprocal absolute temperature in Fig. 3. The results for crystal bar thorium and Ames thorium fall quite well on straight lines. The solubility of thorium dihydride in crystal bar thorium from 300°C to 800°C can be expressed by $\text{Log } C = \frac{1743}{T} + 2.980$, where C is the atomic percent of hydrogen. The temperature dependence of the

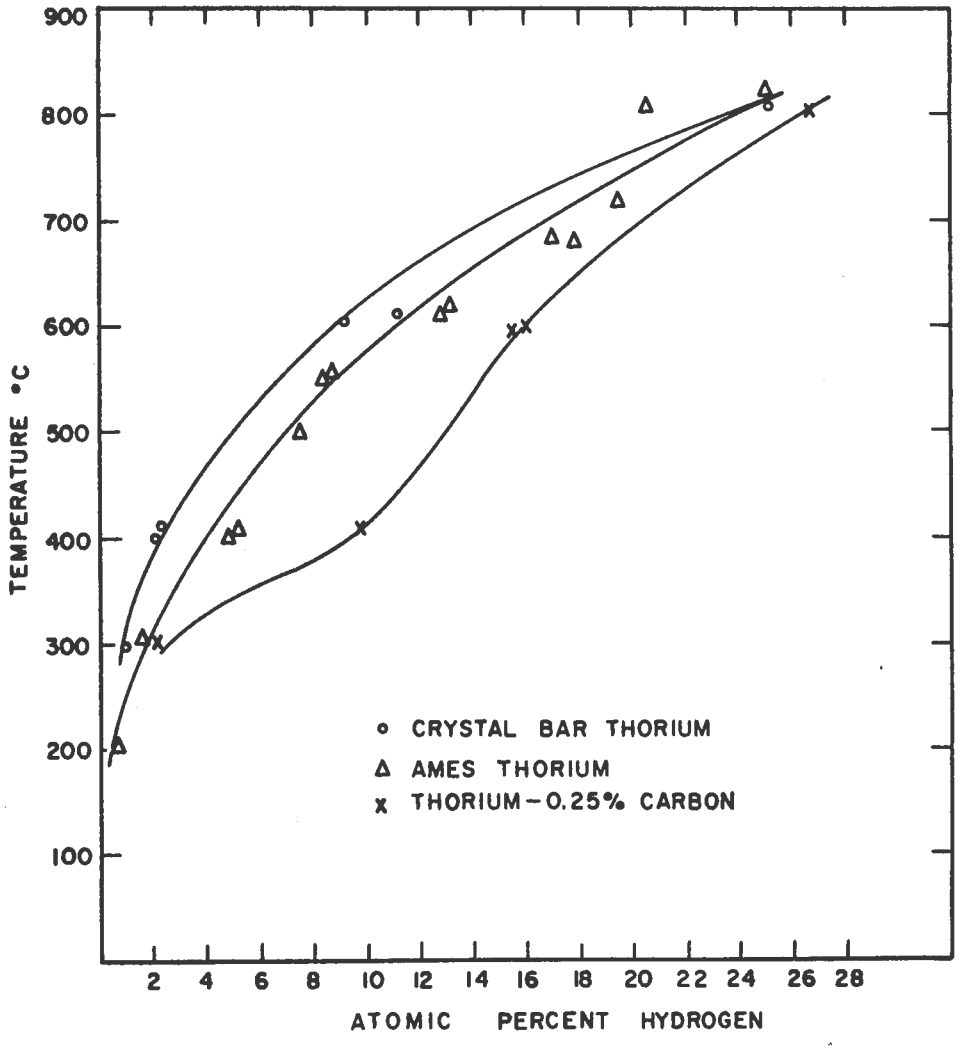

Fig. 2 - The solubility of ThH_2 in thorium at various temperatures. The effect of impurities in increasing the solubility is obvious from the displacement of the curves.

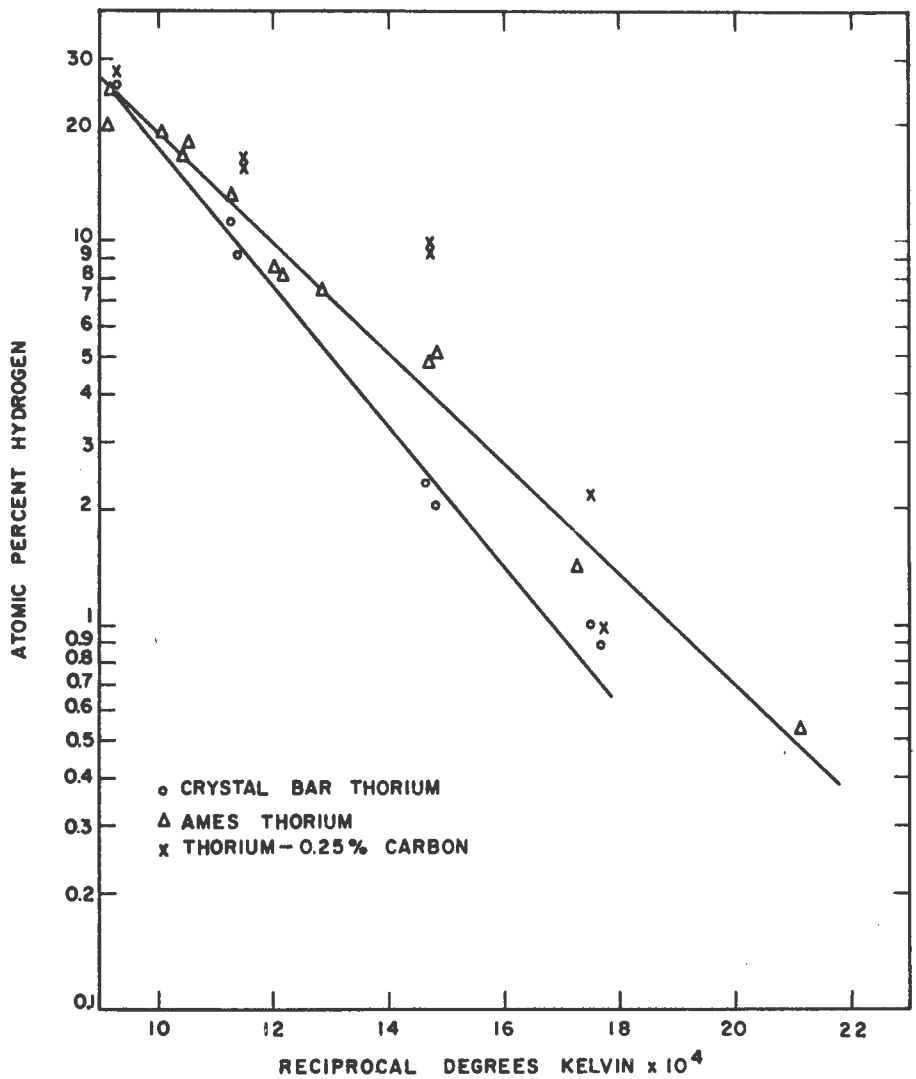

Fig. 3 - Log solubility plotted against reciprocal degrees Kelvin.

solubility gave a value of 8.4 kcal per atom of hydrogen for the heat of solution of thorium dihydride in crystal bar thorium and 6.6 kcal for the heat of solution in Ames thorium. The results of this determination have been presented at the Metal Congress, November 1957, and submitted for publication in the Transactions of the Metallurgical Society of A.I.M.E.

An apparatus has been designed to measure the rate of absorption of hydrogen by thorium metal and also the rate of evolution of hydrogen from thorium metal. The preparation of thorium samples for use in the study of these two reactions has been started.

4.7 Aluminum-Vanadium System (O. N. Carlson, J. F. Smith, and D. M. Bailey)

In view of the recent structural investigations[1,2,3] of the aluminum-vanadium compounds, the aluminum-rich section of the diagram was again investigated. The structural work has shown that the α - and β -phases differ slightly from the formulae proposed by Carlson, Kenney, and Wilhelm.[4] The α-phase does not occur at VAl_{11} but has been shown to vary between the limits VAl_{10} and V_2Al_{21}. The β -phase occurs at

---

1. P. J. Brown, Acta Cryst. 10, 133 (1957).
2. J. F. Smith and A. E. Ray, Acta Cryst. 10, 169 (1957).
3. A. E. Ray and J. F. Smith, Acta Cryst. 10, 604 (1957).
4. O. N. Carlson, D. J. Kenney and H. A. Wilhelm, Trans. Am. Soc. Metals, 47, 520 (1955).

V_4Al_{23} rather than at VAl_6. An additional phase, α', has been found between the α - and β -phases. This compound[1] is monoclinic with the following parameters: a=25.4Å, b=7.59Å, c=11.0Å, and β =127°, and on the basis of chemical analysis and cell dimensions the tentative formula is V_7Al_{45}.

All three of the phases, α, α', and β, form by peritectic reaction temperatures relative to the melting point of aluminum, 660.2°C. The results for two alloys are summarized in Table XI. The thermal arrests for the 6.29 w/o

Table XI. Peritectic Reaction Temperatures for Aluminum-Vanadium Alloys

Reaction	6.29 w/o V	17.14 w/o V
$Al \rightleftharpoons \alpha + L$	661.9°C	- - -
$\alpha \rightleftharpoons \alpha' + L$	668 °C	671°C
$\alpha' \rightleftharpoons \beta + L$	688 °C	680°C
$\beta \rightleftharpoons \gamma + L$	736 °C	735°C

vanadium alloy were considerably sharper than those of the 17.14 w/o alloy because of the difference in the relative amounts of the phases present. This behavior accounts for

1. P. J. Brown, Private communication.

the small differences in the peritectic temperatures reported for the two alloys and makes the values for the 6.29 w/o alloy the more reliable.

4.8 Thorium-Molybdenum System (D. E. Williams and P. E. Palmer)

X-ray diffraction studies of thorium-molybdenum powders, which had been annealed and cooled slowly to room temperature, indicate no detectable solubility at either end of the diagram. Diffraction patterns from both Debye-Scherrer and back-reflection cameras showed no change in the lattice parameters of thorium or molybdenum with changing composition.

4.9 Zirconium-Nickel System (D. E. Williams and M. E. Kirkpatrick)

Metallographic study of water-quenched samples of zirconium-rich alloys has yielded the following information regarding the phase diagram. The maximum solubility of nickel in α - zirconium is of the order of 0.1%, while the maximum solubility of nickel in β - zirconium is 1.9% at 960°C. The following compounds have been located by metallographic as well as melting-point data; $NiZr_2$ - 24.3% Ni, NiZr - 39.3% Ni, Ni_3Zr - 65.9% Ni, and Ni_4Zr - 72% Ni. The compound Ni_4Zr is formed by a peritectic reaction of Ni_3Zr and liquid at 1300°C. Eutectics have been found to occur at 17% Ni - 960°C, 27% Ni - 1010°C, 52 ± 2% Ni - 1060°C, and 87 ± 2% Ni - 1170°C.

A eutectoid reaction occurs as a result of the α to β transformation in zirconium. Metallographic experiments have placed the eutectoid at 1.3% nickel. Electrical resistance data have failed to locate the exact temperature of the eutectoid.

4.10 Thorium-Tantalum System (D. E. Williams and O. D. McMasters)

Results of melting point determinations indicate a eutectic system with the eutectic horizontal at about 1700°C. On the basis of metallographic study, the eutectic composition is thought to be between 20 and 30% tantalum. According to metallographic and X-ray diffraction data, there is no detectable terminal solubility at either end of the diagram at room temperature. The solubility limit of thorium in tantalum is about 5% at 1700°C, while the solubility of tantalum in thorium at this temperature is less than 3%.

4.11 The Uranium-Hafnium System (D. T. Peterson and D. J. Beerntsen)

Thermal analysis and microscopic examination have established the eutectoid at the uranium end of this system. The eutectoid composition is between 3.1 and 6.1 a/o hafnium. The eutectoid temperature is 732°C. Microscopic examination of 97.0 and 98.4 a/o hafnium alloys quenched from 740°C

indicated that these were one-phase α - hafnium alloys. X-ray diffraction patterns from a 24 a/o hafnium alloy in the furnace-cooled condition had only α - uranium and α - hafnium lines.

4.12 The Yttrium-Titanium System (O. N. Carlson, D. Bare and F. H. Spedding)

Yttrium and titanium form a simple eutectic system with limited terminal solid solubility as was described in ISC-903. The eutectic temperature was determined to be 1330°C and the eutectic composition approximately 10 w/o Ti. The solid solubility of titanium in yttrium was estimated from microstructures to be less than 2 w/o Ti at 1350°C. A series of titanium-rich alloys were quenched from 1200, 1350, 1400 and 1450°C in an effort to establish the solubility limit of yttrium in titanium at these temperatures. Because of the difficulties encountered in interpreting the microstructures of these alloys, due apparently to lack of purity of the titanium sponge used, some crystal-bar titanium was prepared. The microscopic appearance of this material was nearly free of inclusions or second phase impurities. Alloys prepared from the crystal bar are now being used in the determination of the limit of solid solubility on the titanium-rich end of the system.

4.13 Molybdenum-Rhenium System (D. E. Williams and W. H. Pechin)

A series of alloys covering the entire composition range of the system has been prepared by arc-melting. The 20% and 30% molybdenum alloys were brittle, and cracked or broke under very little strain. Hardness data and metallographic examination indicate the possibility of the existence of an intermetallic compound near 20% molybdenum which might account for the extreme brittle behavior of the alloys in this composition range.

Alloys of more than 30% rhenium composition were found to be difficult to machine using ordinary tools and methods. All cutting was done with a silicon carbide abrasive saw and these alloys could not be drilled with steel or tungsten carbide drills. The reason for this resistance to machining is probably due to the rapid work hardening of rhenium.

Results from metallographic examination of the as-cast alloys indicate extended solubility of rhenium in molybdenum, about 40% at room-temperature.

4.14 Vanadium-Chromium System (O. N. Carlson and A. Eustice)

The investigation of the vanadium-chromium alloy system has been completed during this report period. As reported

previously (ISC-903) vanadium and chromium form a continuous series of solid solutions at all compositions across the system. There is a minimum in the solidus which occurs at a temperature of 1750°C and at a composition of approximately 70 w/o Cr. Alloys containing 40 w/o Cr and 60 w/o Cr were annealed at 900°C and at 1200°C for 500 hours and 170 hours, respectively, with no microscopic evidence for the existence of an intermediate phase appearing in any of the specimens. The lattice parameters, determined on alloys at 10 percent composition intervals, are presented in Table XII.

Table XII. Lattice Constants of V-Cr Alloys

Composition w/o	Lattice Constant (in Angstroms)
100	2.885
90	2.894
80	2.907
70	2.920
60	2.932
50	2.949
40	2.968
30	2.980
20	2.998
10	3.015
0 (pure V)	3.035

The work on the V-Cr system is scheduled for presentation at the Reactive Metals Conference of the AIME to be held in Buffalo, New York on May 27-29, 1958 and will be published in the Proceedings of that conference.

4.15 Thorium-Vanadium System (D. E. Williams, P. E. Palmer and V. C. Marcotte)

The availability of higher-purity materials has made the reinvestigation of this system desirable. Both the thorium and vanadium used to make the alloys for this investigation were prepared at the Ames Laboratory by the thermal decomposition of the metal iodides.

Melting-point determinations made on thorium-rich alloys place the eutectic at 5.5 ± 1% vanadium and 1415°C.

Some temperature-resistance experiments covering the range from 600°C to 1600°C have been started on the high vanadium alloys. Results from the few runs which have been made indicate the eutectic horizontal extends to at least 99% vanadium. X-ray patterns made from powders of vanadium-rich alloys give no indication of any solubility of thorium in vanadium at room temperature. This observation is corroborated by metallography.

5. Corrosion Studies

5.1 Corrosion Properties of Some of the Refractory Metals and Their Alloys (O. N. Carlson, D. Bare and F. H. Spedding)

The oxidation properties of yttrium-titanium alloys and their behaviour in high temperature water were studied during this period. Oxidation tests were run on a series of alloy specimens at 500° and 800°C in air. The oxidation rate of titanium upon exposure to air at 500°C for 1200 hours was 4.5×10^{-5} mg/cm^2/hr and of yttrium 3.9×10^{-3} mg/cm^2/hr. The results of the tests on the binary alloys indicated that the binary addition of either metal to the other resulted in higher corrosion rates than were obtained on the unalloyed metal. All of the samples tested at 800°C gained more than 1% in weight after 200 hours. Most of the alloys became coated with a red and yellow oxide product which resembled Ti_2O_3 and TiO_3. Neither titanium nor yttrium exhibited this colored corrosion product in the 500°C test but unalloyed titanium was coated with a film of the product after testing at 800°C.

Corrosion tests of the titanium-yttrium alloys in boiling water (100°C) were completed after being run a total of 1000 hours. Yttrium and yttrium-rich alloys became

pitted and exhibited perferential corrosion in some areas of the specimens. The corrosion rate of unalloyed yttrium was found to be 2.0×10^{-2} mg/cm^2/hr and the corrosion rates of the yttrium-rich alloys were similar. Titanium and the titanium-rich alloys exhibited corrosion rates of approximately 1.5×10^{-3} mg/cm^2/hr in the boiling water test.

6. Solid State Investigations

6.1 Physical Properties of $CaMg_2$ and $MgCu_2$ (J. F. Smith and J. R. Ogren)

6.1.1 Electrical Resistivity

Electrical resistivity measurements have been made on single crystals of hexagonal $CaMg_2$ and polycrystals of $MgCu_2$. These two compounds belong to the large group of intermetallic compounds known as Laves phases. Resistivity values were determined by the relatively common method in which the potential drop across the sample is compared with the potential drop across a standard resistance in series with the sample. In these measurements a manganin standard resistor was used, and its resistance as determined with a Leeds and Northrup type K potentiometer. Potential probes were fabricated from 20 mil tungsten wires which were sharpened by repeated dipping in molten potassium nitrite. Current was reversed at each experimental point in order to detect any extraneous effects

due to contact potentials. Specimen dimensions and probe separations were measured with a traveling microscope.

The temperature of the sample was continuously variable from the boiling point of liquid nitrogen to room temperature. This temperature control was achieved by a gas flow technique which has been described by Cioffi and Taylor.[1] Two calibrated iron-constantan thermocouples, one at each end of the sample, were used as thermometers. Comparison of the readings of the two thermocouples showed that, with an occasional exception, the temperature gradient across the sample was zero within the precision of measurement.

Resistivity measurements were made on single crystalline specimens of $CaMg_2$ with current flow both parallel and perpendicular to the unique crystallographic axis. The temperature dependence of these resistivity measurements is shown in Fig. 4. A similar plot of resistivity measurements of polycrystalline $MgCu_2$ is shown in Fig. 5. The plots show no thermal hysteresis. Room temperature resistivities are shown in Table XIII and temperature coefficients of resistivity in Table XIV. The data indicate an appreciable variation in specific resistivities of equivalent specimens.

---

1. P. P. Cioffi and L. S. Taylor, J. Opt. Soc. Am. 6, 906 (1922).

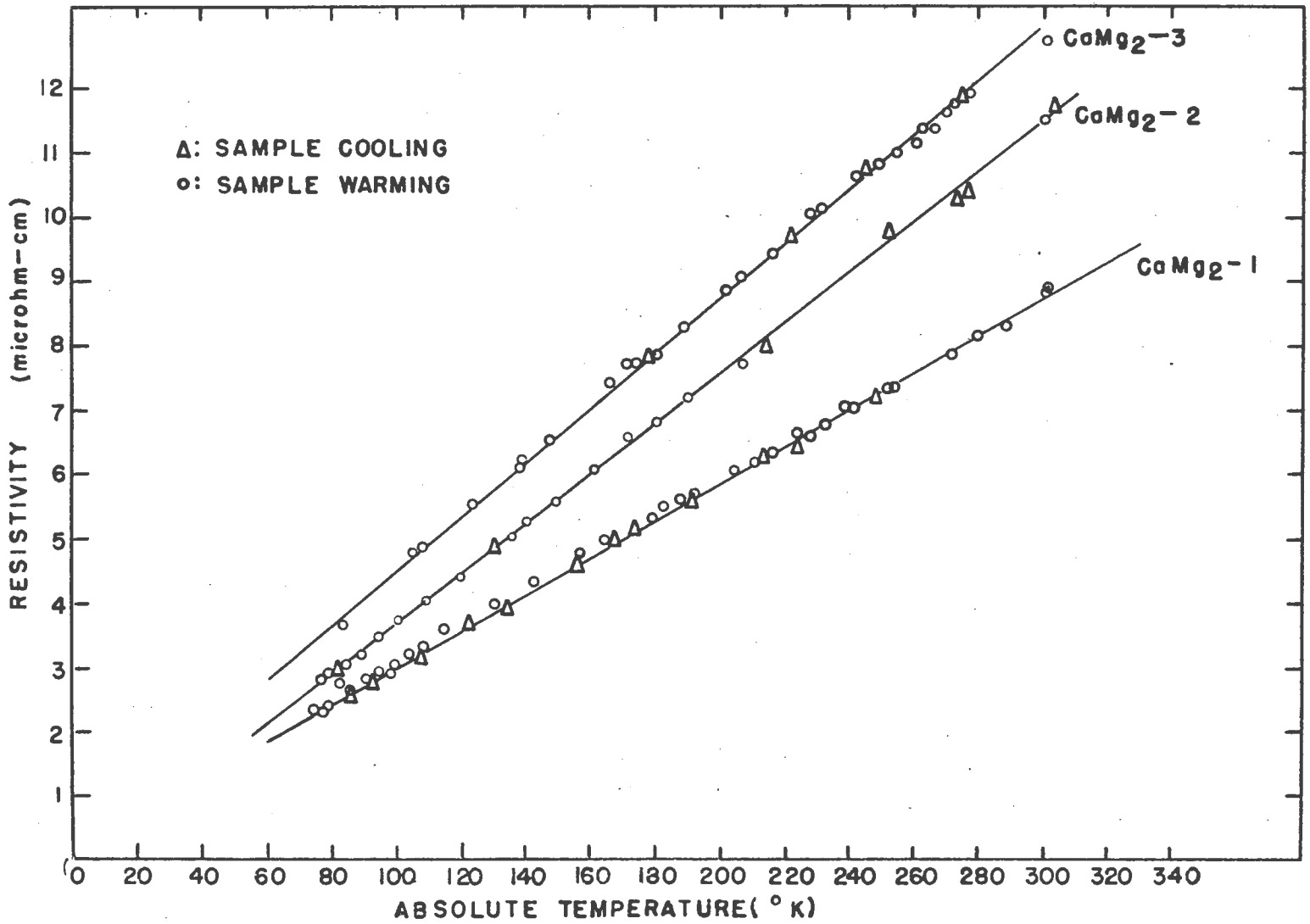

Fig. 4 - Resistivity as a function of temperature for single crystals of $CaMg_2$. Curves 1 and 3 are for current flow parallel to the c-axis. Curve 2 is for current flow perpendicular to the c-axis.

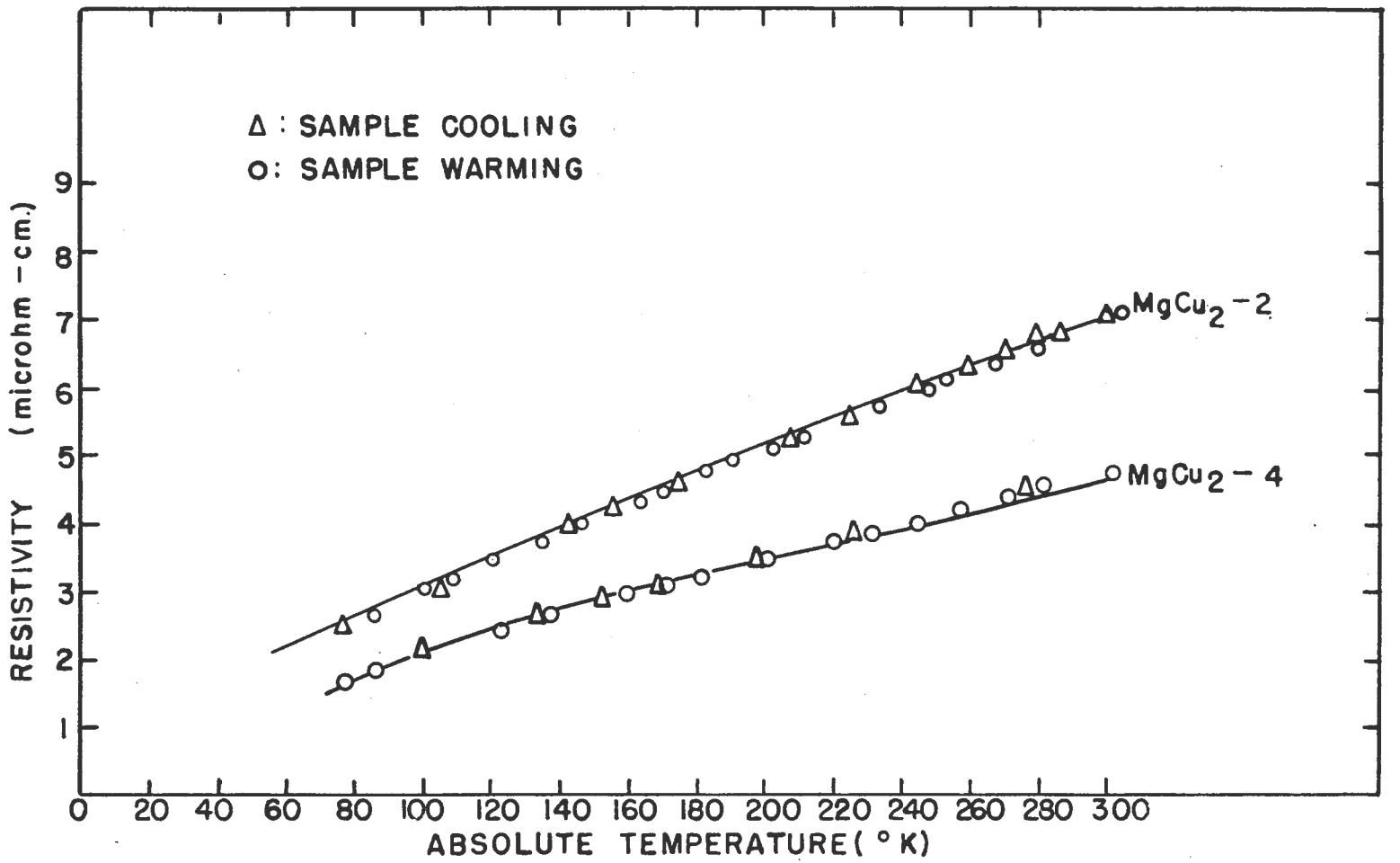

Fig. 5 - Resistivity as a function of temperature for two specimens of polycrystalline $MgCu_2$.

The extreme values differ by almost a factor or two. In contrast the temperature coefficients of resistivity show only a small variation from specimen to specimen. It is believed that the scatter of resistivity values is due primarily to variations in the scattering cross-sections for conduction electrons. This belief is based upon the fact that measured Hall coefficients show that the variation in the effective number of charge carriers is inadequate to account for the observed resistivity variation. In addition the resistance of two specimens of $CaMg_2$ and one of $MgCu_2$ were measured with the sample submerged in liquid helium. These measurements were considerably less precise than the measurements at higher temperatures but the resistivities at 4.2°K were found to be only slightly less than the resistivities at 80°K. Such high residual resistivities indicate appreciable concentrations of impurities or structural imperfections.

Since there should be little variation in impurity content among equivalent test specimens, the differences in resistivity values must be due primarily to differences in structural perfection. One type of imperfection that is possible in compounds but not in pure elements is a local disorder of atoms on the crystallographic sites. As a first

Table VIII. Electrical Resistivities of $CaMg_2$ and $MgCu_2$ at 20°C

Test Specimen	Orientation	Resistivity (microhm-cm)
$CaMg_2$--1	Current parallel c-axis	8.69 ± 0.20
$CaMg_2$--3	" " "	12.84 ± 0.19
$CaMg_2$--3A	" " "	11.9 ± 0.9
$CaMg_2$--4	" " "	16.24 ± 0.32
$CaMg_2$--2	Current perpendicular c-axis	11.73 ± 0.19
$CaMg_2$--5	" " "	18.00 ± 0.36
$MgCu_2$--1A	Unoriented polycrystal	5.40 ± 0.00
$MgCu_2$--2	" "	7.08 ± 0.14
$MgCu_2$--3	" "	6.17 ± 0.12
$MgCu_2$--4	" "	4.80 ± 0.10
$MgCu_2$--5	" "	6.00 ± 0.12
$MgCu_2$--6	" "	4.53 ± 0.09

Table XIV. Temperature Coefficients of Resistivity for $CaMg_2$ and $MgCu_2$

$$\alpha = \frac{\rho(T) - \rho(0°C)}{T\rho(0°C)}$$

Test Specimen		Temperature Coefficient ($deg^{-1} \times 10^3$)
$CaMg_2$--1	Current parallel c-axis	3.64 ± 0.01
$CaMg_2$--3	" " "	3.56 ± 0.01
$CaMg_2$--3A	" " "	3.52 ± 0.01
$CaMg_2$--2	Current perpendicular c-axis	3.70 ± 0.01
$MgCu_2$--2	Unoriented polycrystal	2.96 ± 0.01
$MgCu_2$--4	" "	2.91 ± 0.01

approximation such a misarrangement of atoms might be expected to have about the same effect on electrical resistivity as an interstitial or vacancy.[1] On this basis the number of misfit atoms necessary to account for the observed scatter in resistivity values would be of the order of an atomic percent.

6.1.2 Hall Coefficients

The Hall coefficients were measured by an alternating current method. A frequency of 100 cps was employed. The details of construction and operation of this particular Hall apparatus have been adequately described in previous reports.[2,3] Single crystals of $CaMg_2$ were measured with the following orientation: c-axis parallel to the primary current and perpendicular to the magnetic field; c-axis perpendicular to the primary current and parallel to the magnetic field; c-axis perpendicular to both primary current and magnetic field. Again, only polycrystalline $MgCu_2$ specimens were measured. The results are summarized in Table XV. No dependence of the Hall coefficients upon primary current or

---

1. J. S. Koehler in "Impurities and Imperfections" (Am. Soc. Metals, Cleveland, 1955), p. 162.
2. A. A. Read, C. J. Kevane, and E. B. Harris, U. S. Atomic Energy Commission Report No. ISC-387 (1953).
3. W. R. Gardner and G. C. Danielson, Phys. Rev. 93, 46 (1954).

magnetic field was observed. Currents up to two amperes and magnetic fields up to 10,000 gauss were used. The mean values for the Hall coefficients correspond to carrier densities of 0.67 electrons/atom for $MgCu_2$ and 0.83 'holes'/atom for $CaMg_2$ if a one band model is assumed.

Table XV. Hall Coefficients at Room Temperature

Test Specimen	Orientation	Hall Coefficient (cm^3/coulomb) x 10^4
$CaMg_2$--5	current parallel c-axis magnetic field perpendicular c-axis	+ 2.34 ± 0.17
$CaMg_2$--6	current perpendicular c-axis magnetic field perpendicular c-axis	+ 2.24 ± 0.15
$CaMg_2$--6	current perpendicular c-axis magnetic field parallel c-axis	+ 1.92 ± 0.14
$MgCu_2$--5	unoriented polycrystal	- 1.29 ± 0.09
$MgCu_2$--6	" "	- 1.41 ± 0.10

6.1.3 Thermal Coefficients of Expansion

The thermal coefficients of expansion of $CaMg_2$ and $MgCu_2$ were measured in the temperature range 80-300°K. Precision lattice parameters were measured as a function of temperature by means of X-ray diffraction. A modified Norelco X-ray

diffractometer was employed. Temperature was controlled to ± 2°C by passing a pre-cooled gas through a copper sample holder. Temperatures were measured with a copper-constantan thermocouple in direct contact with the polycrystalline sample. The region around the sample holder and sample was evacuated in order to provide thermal insulation. Precision parameters were obtained by extrapolating values calculated from individual X-ray reflections against the Nelson-Riley function.[1] The precision lattice parameter as a function of temperature for $MgCu_2$ is shown in Fig. 6. For $MgCu_2$ a value of $(30.00 \pm 0.06) \times 10^{-6}$ per °C was obtained for the linear coefficient of thermal expansion. This value was obtained by making a linear fit to the observed points by the method of least squares. For $CaMg_2$ values of $(48.3 \pm 0.3) \times 10^{-6}$ per °C parallel to the c-axis and $(44.4 \pm 0.1) \times 10^{-6}$ per °C perpendicular to the c-axis were obtained. The lower precision observed in the hexagonal $CaMg_2$ arises from the fact that two lattice parameters were obtained from each diffraction pattern while only a single lattice parameter was obtained from each diffraction pattern for the cubic $MgCu_2$.

---

1. J. B. Nelson & D. P. Riley, Proc. Phys. Soc. (London) 57, 160 (1945).

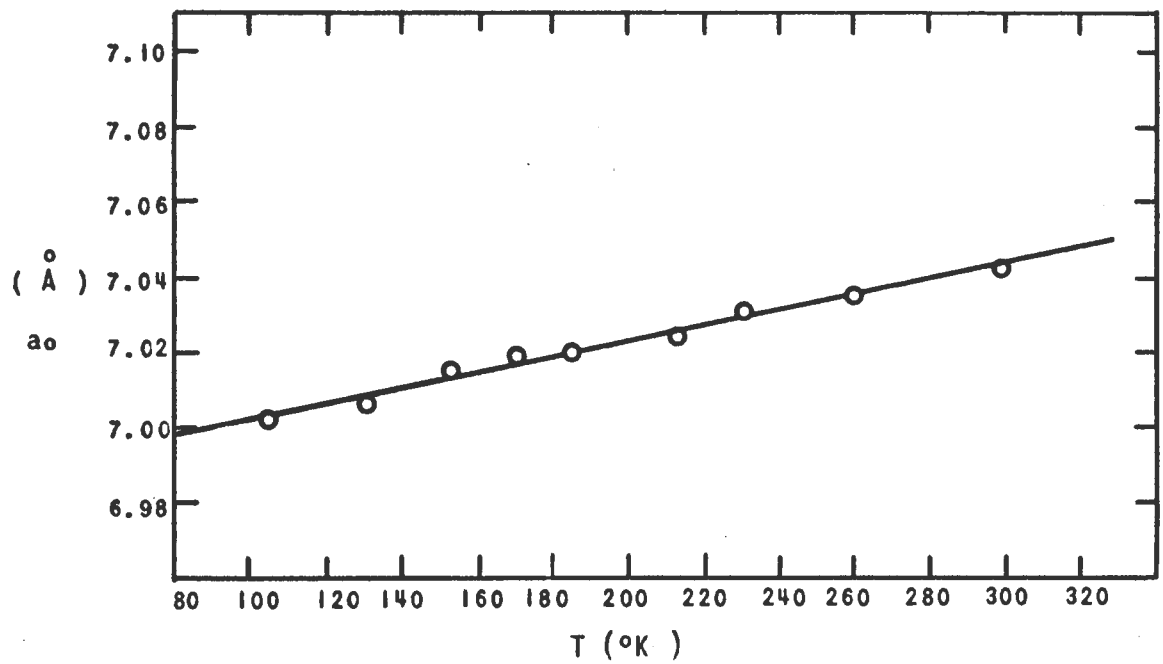

Fig. 6 - Lattice parameter as a function of temperature for $MgCu_2$.

6.2 Effects of Impurities on the Allotropy of Calcium

(J. F. Smith and B. T. Bernstein)

Previous work at this laboratory[1] has shown that the allotropic behavior of calcium metal is affected by minor impurity contamination. In the present investigation high-purity calcium was deliberately contaminated with impurities. Analysis of the calcium before contamination showed the following impurity content: Mg, 0.01 w/o; N, 0.01 w/o; C, 0.02 w/o; and Si, 0.005 w/o. Ba, Be, B, Fe, and Al were spectroscopically estimated to be present in quantities less than 0.001 w/o and Cd, Cu, K, and Li were present to less than 0.0001 w/o. No other metallic impurities were detected. This calcium differs slightly in impurity content from that studied previously.[1] These differences are shown in Table XVI.

Table XVI

Element	Analysis of Ca used in previous work	Analysis of Ca used in present work
C	no analysis	0.02
Fe	0.01 w/o	< 0.001 w/o
Mn	0.005 w/o	< 0.001 w/o
Si	trace	< 0.005 w/o
Ba	not detected	< 0.001 w/o

1. J. F. Smith, O. N. Carlson, and R. W. Vest, J. Electrochem. Soc. 103 409 (1956).

Elements not listed in Table XVI either showed no variation in content or were not determined.

The small difference in impurity content was sufficient to cause a difference in allotropic behavior. In the original investigation pure calcium was found to exist in only two forms: f.c.c. up to 464°C and b.c.c. above 464°C. In the present investigation diffraction patterns taken at 18°, 168°, 207°, and 248°C showed only the f.c.c. phase. Patterns taken at 380° and 419°C showed a coexistence of the f.c.c. and h.c.p. phases. At 575° and 595°C only b.c.c. peaks were observed. This behavior was reproducible from sample to sample and reversible in temperature with the following observations. Patterns taken at 500°C after slowly cooling from 575-595°C showed only h.c.p. reflections. Rapid cooling to 500°C showed an initial persistence of the b.c.c. phase which transformed to the h.c.p. phase in approximately five minutes. This observation was made by scanning over a limited arc in the front reflection region to observe the appearance or disappearance of the strong reflections from each phase. The coexistence of h.c.p. and f.c.c. phases and the sluggish transformation of b.c.c. to h.c.p. suggest that the h.c.p. is not an equilibrium phase of pure calcium.

The elements most logically suspected as causes for the difference in behavior of the present calcium and the original calcium are carbon, oxygen, or hydrogen. For this reason deliberate contamination of the calcium with these elements was undertaken. Nitrogen was included in the list of contaminants because it was believed to be responsible for the low symmetry phase previously observed in less pure calcium.[1]

6.2.1 Contamination with Ethane

Contamination with gaseous species was accomplished by connecting a 200 ml bulb of the gas to the system and subsequently opening the stopcock to allow the contaminant to diffuse into the system at the desired time. Ethane was introduced into the system at room temperature. A diffraction pattern showed only the f.c.c. phase. The specimen was then heated to 490°C for one hour to allow reaction. At the end of this time a diffraction pattern taken at 490°C showed only h.c.p. reflections. Cooling to room temperature revealed a coexistence of f.c.c. and h.c.p. This coexistence persisted for at least four hours after which time the sample was again heated. A pattern at 180°C showed f.c.c. plus h.c.p. Patterns

---

1. J. F. Smith, O. N. Carlson, and R. W. Vest, J. Electrochem. Soc. 103 409 (1956).

at 235°, 265°, 300°, and 331°C showed three phases: f.c.c., h.c.p., and the low symmetry phase. A pattern at 395°C showed only h.c.p. It was observed that the intensity of the f.c.c. reflections decreased with increasing temperature while the h.c.p. reflections and the reflections of the low symmetry phase increased in intensity with increasing temperature. The behavior was reversible.

6.2.2 Contamination with Carbon

In an attempt to separate the effects of carbon and hydrogen the calcium was contaminated with Mallinckrodt #4392 charcoal powder. This powder was sprinkled on a file and the sample was inverted and lightly abraded across the file until a thin adherent film of carbon had collected on the sample. Diffraction patterns taken at intervals between room temperature and 326°C showed f.c.c. only. Patterns at 380° and 513°C showed h.c.p. only. Patterns at 550° and 575°C showed b.c.c. only. Subsequent rapid cooling to room temperature caused the appearance of reflections of the low symmetry phase in coexistence with f.c.c. This coexistence persisted in patterns up to 300°C. At 321° and 375°C only the low symmetry phase appeared; at 386° and 513°C only h.c.p. appeared; and at 565°C only b.c.c. appeared. A final check at room temperature showed the low

symmetry phase and f.c.c. coexisting. This coexistence persisted for at least 96 hours after which time the run was discontinued.

6.2.3 Contamination with Nitrogen

Nitrogen was introduced into the system at 321°C. A diffraction pattern showed the immediate appearance of the low symmetry phase coexisting with the f.c.c. which was initially present. At lower temperatures f.c.c. appeared alone. Patterns at 386°C and 486°C showed h.c.p. only and at 575°C b.c.c. only. The behavior was reproducible and reversible. It should be noted that the penetration of the contaminant into the sample was greater than in the original work. In this case an attempt to restore the calcium to its initial behavior by filing off the surface layer was unsuccessful.

6.2.4 Contamination with Oxygen

Oxygen was added to the system at 321°C. For this experiment the tantalum heating element was replaced by platinum and the furnace mounts and shields were replaced with copper. Repeated runs revealed only the most intense oxide reflections plus the patterns observed in the uncontaminated calcium at equivalent temperature. The low symmetry phase was not observed at any temperature.

6.2.5 Summary and Comments

On the basis of these results it seems that oxygen is not responsible for the appearance of either the h.c.p. or the low symmetry phase. Nitrogen is unquestionably capable of inducing the appearance of the low symmetry phase. Carbon also seems capable of inducing the appearance of the low symmetry phase, but the possibility of simultaneous contamination by nitrogen adsorbed on the powdered carbon cannot be ruled out at present. However, the persistence of the low symmetry phase to room temperature after carbon and ethane contamination but not after nitrogen contamination makes carbon a definite possibility. It is planned to make similar measurements with boron contamination to determine whether the stabilization of the low symmetry phase is an effect associated with interstitial atoms. The only contaminant which affected the range of stability of the h.c.p. phase was ethane. This implies that hydrogen may be responsible for the stabilization of the h.c.p. structure. An attempt will be made to verify this supposition.

6.3 Growth of Small Spherical Crystals of Metals and Alloys (J. F. Smith and A. E. Ray)

In the determination of crystal structures, precise measurements of the intensity of diffraction peaks are necessary for resolution of detail. Such intensity measurements

must be corrected for absorption effects. These corrections are most easily made on crystals of simple geometric shape such as spheres and cylinders. The method of crystal growth to be described here produces small single crystals which are nearly perfect spheres. Further, crystals of several different diameters are produced in one operation, and intensity data taken from crystals of different size gives information concerning the relative importance of primary and secondary extinction effects.

A spherical shape may be obtained with relative ease since the surface tension of a liquid droplet tends to force it into the form of a sphere. The problem is to induce solidification without distortion of shape and with the constraint that the rate of formation of nuclei be small compared with the rate of growth of a nucleus so that an appreciable number of single crystals will result. Splitstone[1] obtained spherical single crystals of lithium by melting small pieces of the metal in paraffin and allowing the resulting globules to solidify. There is an obvious temperature limitation in extending the technique to other materials. Cech and Turnbull[2] prepared spherical single crystals of an

---

1. P. L. Splitstone, Doctoral Thesis, The Ohio State University, Columbus, Ohio.
2. R. E. Cech and D. Turnbull, J. Metals 8, 124 (1956).

iron-nickel alloy in a type of shot tower. Their technique should be applicable to many materials but necessitates the construction of special apparatus.

The present technique utilizes an arc melter which is a relatively common piece of equipment in metallurgical research laboratories. In this method the arc is struck to the sample in short bursts so that the sample is spattered in the form of spherical beads. Some success was achieved when using solid buttons of metal, but best results were obtained when the metal was loaded as a pile of chips or flakes. The melting was done in a water-cooled copper pot under a helium atmosphere. Prior removal of contaminating gases was accomplished by successive evacuation and flushing with helium. The intensity of the arc from the tungsten tipped electrode was adjusted so that the sample was easily melted but without excessive superheating.

Samples of beryllium, vanadium, iron, zirconium, a 70 w/o Ni - 30 w/o Cu solid solution alloy, and the intermetallic compound NiAl were tried. X-ray examination showed that in all materials some of the spheres gave diffraction patterns typical of single crystals; however, no exhaustive check was made to prove the absence of coherent boundaries which could conceivably result from solid state transitions in iron and

zirconium. As might be expected, a much higher proportion of smaller spheres than larger spheres were found to be single crystals. Approximately 50% of the spheres with diameters less than 0.1 mm were found to be single crystals while only 5 to 10% of the 0.5 to 1.0 mm spheres were single crystals. The largest crystal which was obtained was a beryllium sphere 1.5 mm in diameter. In some of the larger crystals a slight flattening on one side of the sphere indicated solidification while stationary with respect to the pot. However, with the Cu-Ni alloy which wets Cu, it is believed that solidification occurred as the beads rolled across the pot.

6.4 Measurements of Elastic Constants of Metal Single Crystals (O. N. Carlson and S. Epstein)

The elastic constants of single crystals of several copper-nickel alloys were determined at room temperature using the pulse-echo technique. Single crystals of pure nickel, of alloys containing 7, 21, 24, 38 a/o Cu, and of pure copper were cut for orientations of $\langle\bar{1}00\rangle$ and $\langle\bar{1}10\rangle$ and propagation velocities of shear and longitudinal waves were measured for each crystal. The longitudinal velocities were compared with those obtained by a resonance method on identical crystals in order to determine a transit time

correction for the pulse-echo method. Attempts are now being made to determine the transit time correction for both the longitudinal and shear waves using a varying crystal thickness method. The three elastic constants, C_{11}, C_{12}, and C_{44}, will then be calculated from the corrected velocities and plotted as a function of composition.

6.5 Low Temperature Properties of Vanadium (O. N. Carlson and B. A. Loomis)

The investigation of a brittle-ductile transition in vanadium was continued and the results have been described in detail in the Doctoral Thesis of B. A. Loomis entitled "Brittle-Ductile Transition in Vanadium". This work will soon be published in a separate report, ISC-1037. The results of this investigation are scheduled for presentation at the Reactive Metals Conference of the AIME to be held in Buffalo, New York on May 27-29, 1958, and will be published in the Proceedings of that Conference.

A brittle-ductile transition was observed in bomb-reduced vanadium metal (99.7+ per cent) at -65°C ± 10°C. A similar transition was observed in crystal-bar vanadium (99.9+ per cent) at -110° ± 10°C. Vanadium was found to regain some of its ductility at temperatures below -140°C. Curves showing the reduction in area and elongation as a

function of temperature (see Fig. 7) show an abrupt drop in ductility for the two grades of vanadium at their respective transition temperatures.

Additions of small amounts of chromium, molybdenum, tantalum and titanium have anomalous maxima and minima effects on the transition temperature of vanadium as is shown by the data plotted in Fig. 8. All of these metals, which form extensive solid solutions with vanadium at room temperature, generally tend to raise the transition temperature markedly. Thorium had little or no effect upon the transition temperature and zirconium had no effect at compositions below that at which appreciable amounts of V_2Zr are formed. The transition temperature was particularly sensitive to the presence of the non-metallic elements, hydrogen, nitrogen and oxygen. The effect of carbon was somewhat less. The effects that the non-metallic elements have upon the brittle-ductile transition are shown by the curves in Fig. 9.

Changes were observed in lattice constant, electrical resistance and internal friction through the transition temperature range. X-ray diffraction data, however, indicated that there is no allotropic transformation down to -180°C.

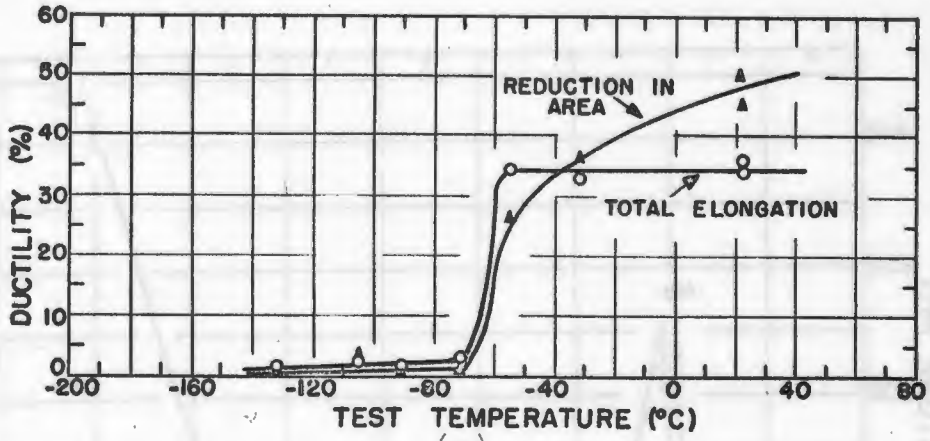

(a)

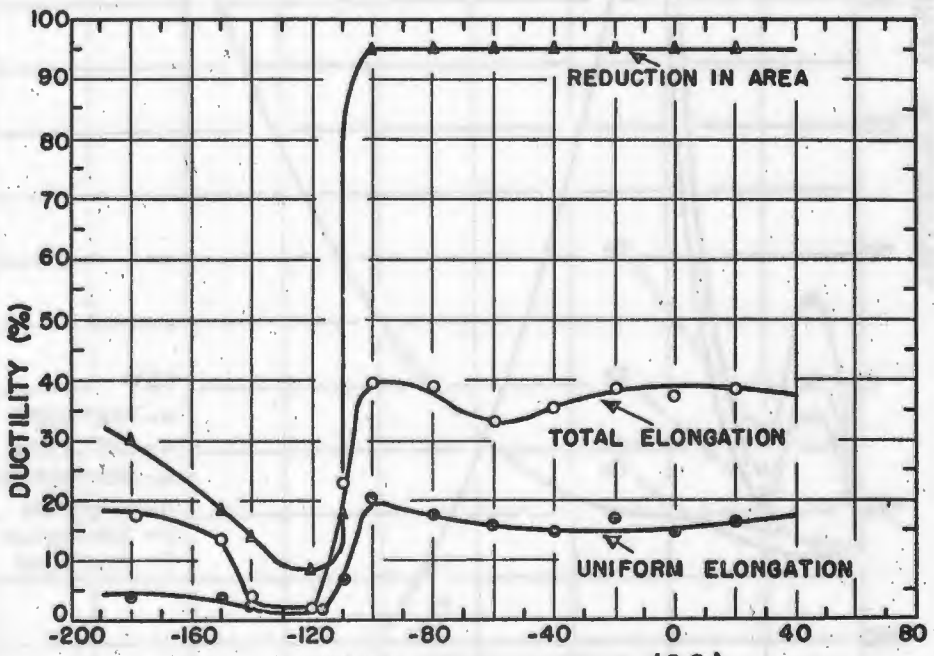

(b)

Fig. 7 - Tensile properties of vanadium as a function of temperature.
(a) Bomb-reduced vanadium
(b) Crystal bar vanadium

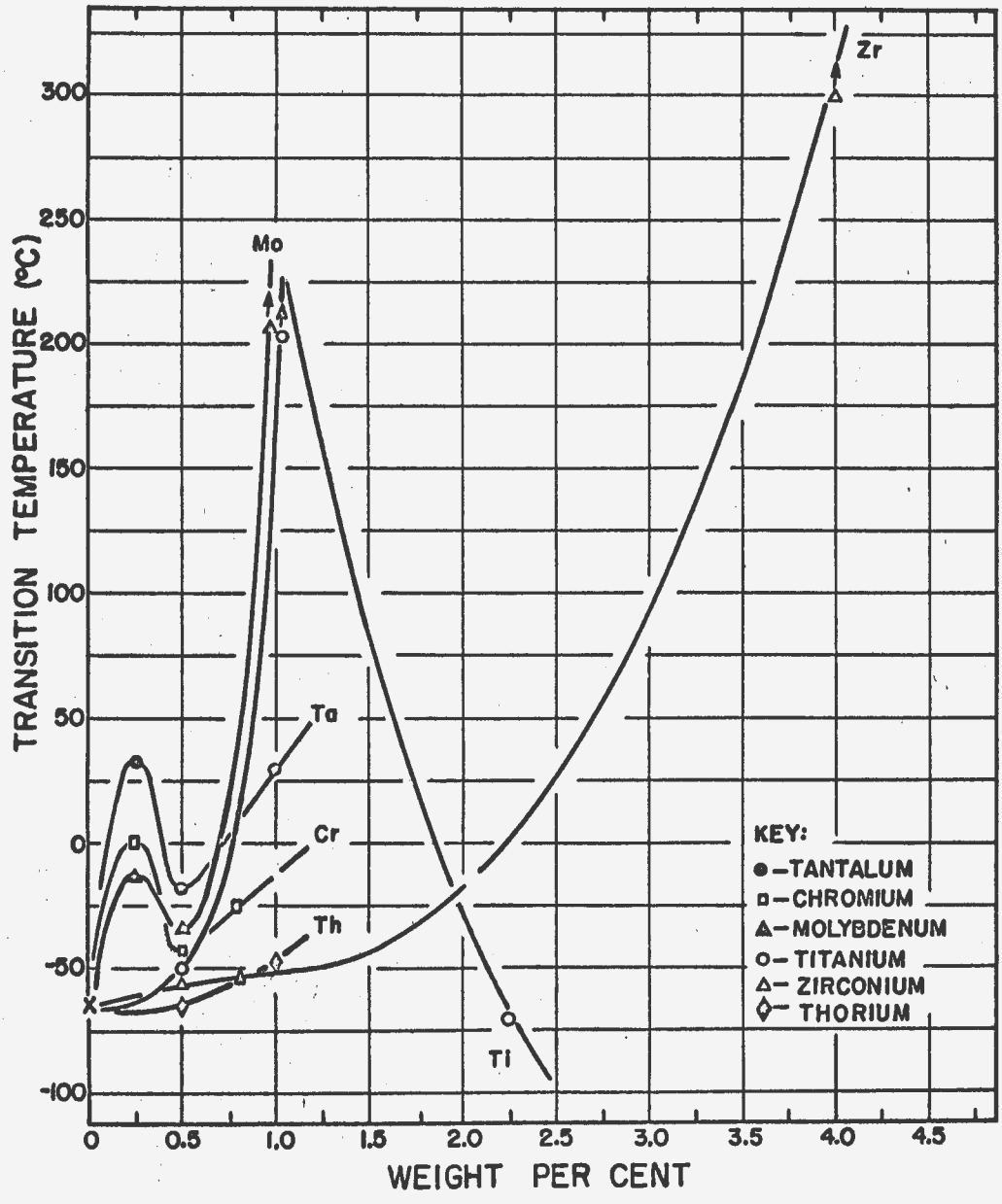

Fig. 8 - Effects of small amounts of metallic elements on the brittle-ductile transition temperature of vanadium.

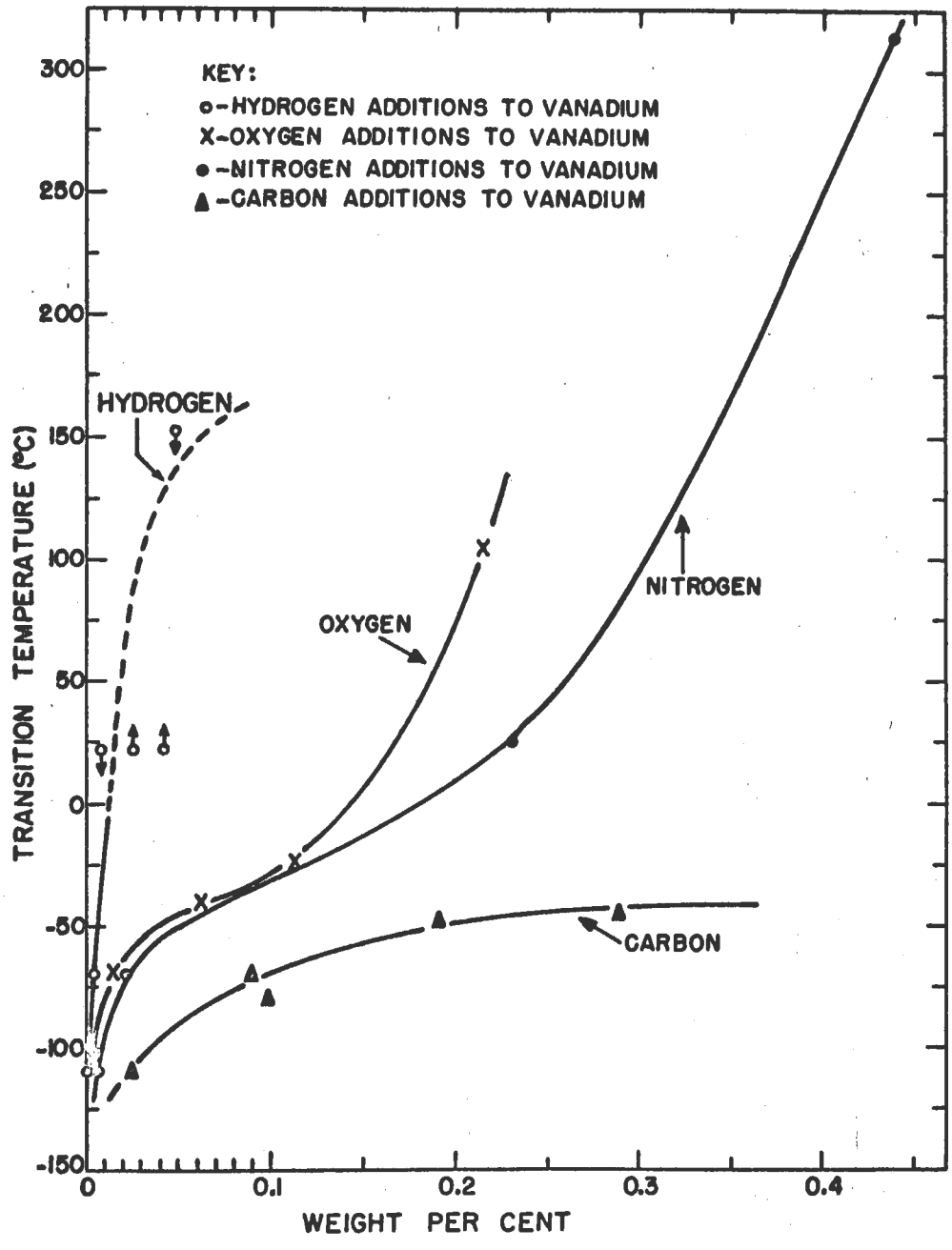

Fig. 9 - Effect of non-metallic elements on the brittle-ductile transition in vanadium.

A continuation of the investigation of this problem includes a detailed study of the effect of hydrogen upon the brittle-ductile transition temperature. These effects will be studied by internal friction measurements, tensile tests and the measurement of other physical properties through the transition temperature range with particular emphasis upon the region of increasing ductility below -140°C. Additional studies are under way on the examination of the effects of extensive substitutional alloying on the brittle-ductile transition.

7. Other Investigations

7.1 Vacuum Fusion Analysis of Metals (D. T. Peterson and M. Indig)

A series of yttrium samples from the same lot of metal were heated in known amounts of oxygen to prepare samples with known additions of oxygen. These samples were analysed by vacuum fusion using a nickel bath. The amount of oxygen added and the amount recovered by vacuum fusion analysis are reported in Table XVII. The percentage of the oxygen added which was found by analysis was quite close to the percentage which was found for lanthanum. The average deviation of the results was 3.2%. This method of analysis appears to be satisfactory for the determination of oxygen

in yttrium if the results are corrected for the incomplete recovery of oxygen.

Table XVII. Recovery of Oxygen in Vacuum Fusion Analysis of Yttrium

Moles of O_2 Added	Moles of O_2 Found	Percentage
3.63×10^{-4}	3.35×10^{-4}	92.3
3.48 "	3.24 "	93.1
3.69 "	3.08 "	83.4
4.28 "	3.79 "	88.4
2.36 "	2.19 "	92.8
2.10 "	1.95 "	92.9
4.62 "	4.05 "	87.7
1.98 "	1.90 "	96.0
	Average	90.1

The preparation of a series of yttrium samples to which known amounts of nitrogen are added has been started. It was found to be necessary to use temperatures of about 1300°C to obtain reaction with nitrogen and even at this temperature the reaction was often incomplete. These samples will be analysed by vacuum fusion to determine the recovery percentage for nitrogen.

7.2 Reaction of Barium with Calcium Chloride (D. T. Peterson, J. A. Hinkebein and E. W. Johnson)

The reaction of barium with calcium chloride is being studied at 900°C. The metal and salt phases are immiscible at this temperature and the composition of the equilibrium phases are being determined by analysis of quenched samples. The results of a number of runs are given in Table XVIII. The composition of each phase is expressed by the mole fraction of total barium and the mole fraction of metal dissolved in the salt or of salt dissolved in the metal. The mole fraction of total calcium would be one minus the mole fraction of barium. The concentrations of $CaCl_2$ and $BaCl_2$ in the salt phase and of calcium metal and barium metal in the metal phase could not be determined since only the total barium and total calcium in each phase was given by the analysis. Hence, in calculating the concentration quotients, the mole fraction of total barium and total calcium in each phase was used as the concentration of $BaCl_2$ and $CaCl_2$ in the salt phase and barium and calcium in the metal phase. The concentration quotients were quite constant over the concentration range studied and did not show a systematic variation with concentration. The solubility of metal in the salt phase was slightly lower for salt compositions from

0.76 to 0.92 mole fraction barium than for the Ca-$CaCl_2$ binary. The solubility of salt in the metal phase was also lower in the ternary compositions than for either binary system.

Table XVIII. Equilibrium Compositions at 900°C

Salt Phase		Metal Phase		Concentration Quotient
N_{Ba}	N_{Metal}	N_{Ba}	N_{MCl_2}	
1.00	0.160	1.00	0.052	---
0.920	0.0326	0.081	0.0056	130
0.905	0.0329	0.081	0.0036	108
0.896	0.0314	0.063	0.0038	128
0.887	0.0393	0.063	0.0042	117
0.884	0.0369	0.044	0.0038	113
0.849	0.0276	0.038	0.0044	122
0.789	0.0615	0.027	0.0048	94.7
0.763	0.0358	0	0.0050	116
0	0.0380		0.0102	---

7.3 Distribution of Silver Between Liquid Lead and Liquid Zinc (D. T. Peterson and R. Kontrimas)

The distribution coefficient for silver between liquid lead and liquid zinc at 500°C has been determined from 0.01 w/o

silver in zinc to 0.7 w/o silver in zinc. The results indicate that at the lower silver concentration the value of the distribution coefficient is about 80 and that it decreases with increasing silver concentration. However, a few of the results have deviated considerably from the values obtained for only slightly different compositions. The most probable experimental error is the inclusion of zinc in the lead sample. In sampling, the pipette with the sintered glass filter must be inserted through the zinc phase to reach the liquid lead and a small amount of zinc could be entrapped. The design of the pipette has been changed to reduce the possibility of including any zinc in the lead sample.

7.4 Fabrication Properties of Yttrium Metal (O. N. Carlson, E. D. Gibson and F. H. Spedding)

The mechanical working properties of yttrium metal have been investigated by cold-rolling, hot-rolling and swaging methods. From cold-rolling tests on vacuum arc-melted yttrium, reductions in thickness from 20 to 90% were obtained depending primarily upon the dimensions of the original section. A thin section can be cold-rolled extensively with only edge cracking and severe cold-working resulting, whereas a thicker bar fails completely after

about 25% reduction. Metallographic observations noted on cold-rolled specimens indicate that the primary cause of cracking is the presence of hard, non-metallic inclusions in the metal. These inclusions apparently act as points of stress concentration where a crack initiates and is propagated transgranularly across the grain.

In all cases after cold-rolling, the metal became brittle even when the reduction in thickness was quite small. Hardness measurements taken at intervals during the cold-working process indicate that the hardness increases from an original value of Rockwell E 60 to a value of E 85 after 7% reduction and to E 93 after 20% reduction. The original hardness was restored by vacuum annealing above 800°C.

Yttrium sheet was fabricated by the use of the following rolling procedure. An yttrium bar was sealed in a wrought-iron jacket and this assembly was hot-rolled into a plate at 800°C. There was no evidence of surface cracking. The iron jacket was removed and the plate was annealed in vacuum at 1000°C for one hour. This plate was then cold-rolled into a thin sheet which was again vacuum annealed in order to obtain a ductile sheet. Attempts to hot swage yttrium were also successful. An yttrium rod was jacketed in a wrought-iron pipe and the assembly was swaged at 800°C

to the approximate size desired. A heat treatment procedure similar to that for hot-rolling was followed. A rod approximately one-eighth inch in diameter and two feet in length was fabricated.

Because of the apparent deleterious effects of the inclusions in yttrium metal upon its cold working properties, an attempt was made to isolate and identify this phase. Yttrium metal was dissolved in a bromine-ethyl alcohol solution, leaving behind the non-metallic impurities as an insoluble residue. An X-ray diffraction pattern of this residue was indexed and the major phase was identified as Y_2O_3. A few weak lines of the pattern were tentatively identified as βYOF.

7.5 Reduction of Vanadium Oxides (R. E. McCarley and W. J. Magruder)

In connection with the interest of this Laboratory in the preparation of metals by carbon reduction of metallic oxides, some work was performed with the reaction of V_2O_5 with carbon in the temperature range 350-1000°C. The purpose of this work was to determine the stoichiometry of the reaction and to study the factors affecting it. At temperatures below 1000°C the reduction of V_2O_5 proceeded only to V_2O_3 in the presence of an excess of carbon and

1 atmosphere pressure. Below 500°C the reaction was impractically slow but at higher temperatures the rate increased rapidly. During the initial stages of the reaction if the temperature was allowed to reach 690° the rate became so rapid that the solids were suddenly blown from the reaction chamber. Determination of both CO_2 and CO for reaction mixtures containing excess carbon in the temperature range 600-700°C showed that the CO_2/CO ratio varied from 105 to 40 in the initial stages of the reaction and decreased to 20 to 40 during final stages of the reduction. Efforts to demonstrate reproducible CO_2/CO ratios and hence reproducible stoichiometry for identical reaction mixtures and conditions indicated only that such cannot be attained. The conclusion must be drawn, therefore, that if vanadium metal is to be prepared from an oxide-carbon reaction, V_2O_3 is a much better choice than V_2O_5 since the reduction of V_2O_3 proceeds only above 1000°C. At these temperatures CO_2 becomes thermodynamically unstable and hence a less complicated reaction stoichiometry should result.

7.6 Vapor Pressure Measurement over Calcium, Magnesium, and Calcium-Magnesium Alloys (J. F. Smith and R. L. Smythe)

Vapor pressures over solid calcium have previously been

measured by Rudberg,[1] Pilling,[2] Douglas,[3] Tomlin,[4] and Priselkov and Nesmeyanov[5] and over liquid calcium by Hartmann and Schneider.[6] The results of these past measurements are plotted together with the present measurements in Fig. 10; the results of Pilling, Douglas, and Tomlin are plotted as a single line in the manner of Tomlin. Analysis of the calcium used in the present investigation showed the following impurity content: Mg, 0.01 w/o; N, 0.01 w/o; C, 0.02 w/o; and Si, 0.005 w/o. Ba, Be, B, Fe, and Al were spectroscopically estimated to be present in quantities less than 0.001 w/o and Cd, Cu, K, and Li were present to less than 0.0001 w/o. No other common metallic impurities were detected.

No single reason seems adequate to account for the lack of agreement shown by the available data. Rudberg's data are obviously low and may be discounted on the basis of the geometry of his effusion vessel and the placement of his heating element. The calcium used by Pilling was quite impure and was reported to contain 1.62% Mg and 1.25% $CaCl_2$. The presence of the magnesium would be expected to lead to

---

1. E. Rudberg, Phys. Rev. 46, 763 (1934).
2. N. B. Pilling Phys. Rev. 18, 362 (1921).
3. P. E. Douglas Proc. Phys. Soc. (London), 67B, 783 (1954).
4. H. Tomlin ibid., 787 (1954).
5. Y. Priselkov and A. Nesmayanov, Doklady Akad. Nauk S.S.S.R. 95, 1207 (1954).
6. H. Hartmann and R. Schneider, Z. anorg. allgem. Chem. 180, 275 (1929).

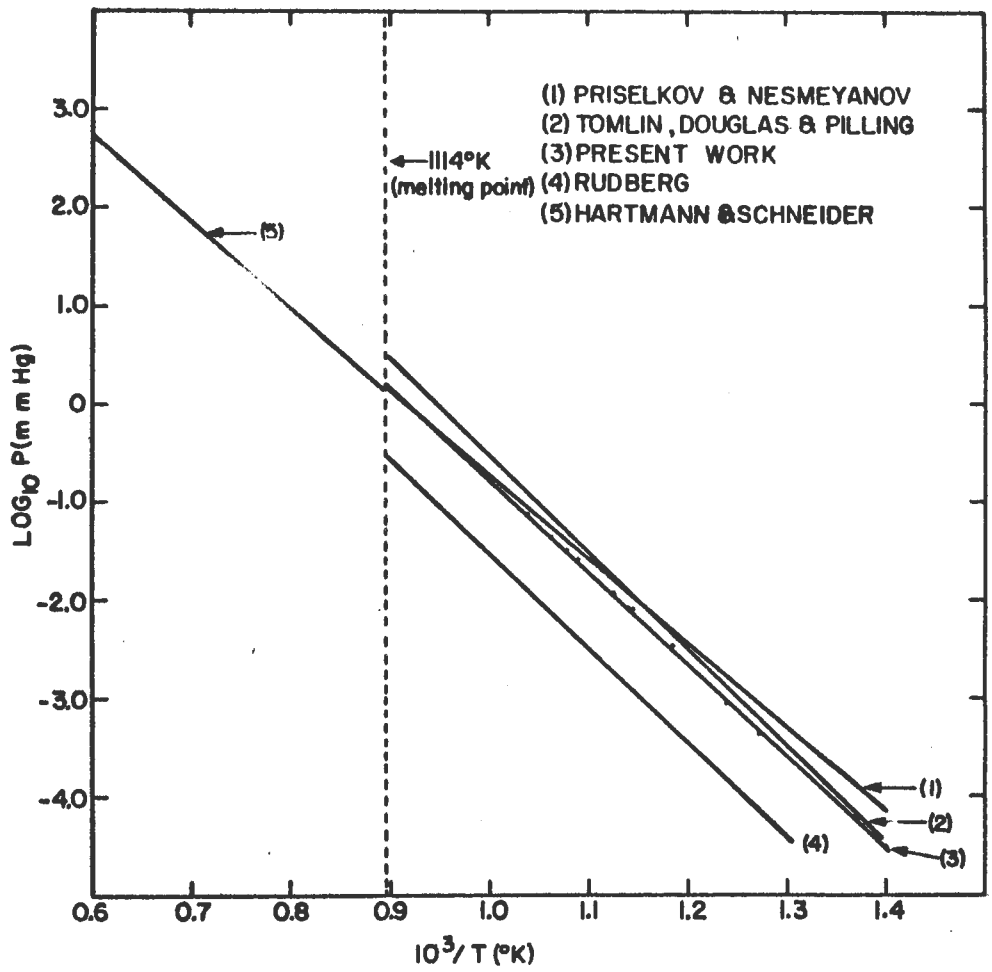

Fig. 10 - Log vapor pressure versus reciprocal temperature as determined by various investigators for calcium.

abnormally high values for the measured vapor pressures. In addition the technique employed by Pilling is susceptible to large experimental errors. Hence, as Tomlin has stated, the agreement between Pilling's results and those of Douglas and Tomlin is quite possibly fortuitous.

No such obvious criticisms are apparent for the work of Douglas, Tomlin, Priselkov and Nesmeyanov, and Hartmann and Schneider. Extrapolation of the data of Priselkov and Nesmeyanov gives a vapor pressure at the melting point in good agreement with the data of Hartmann and Schneider. However, the two sets of data are inconsistent in that the change in slope across the melting point would necessitate an exothermic fusion process. In contrast, comparison of the data of Douglas and Tomlin with the data of Hartmann and Schneider gives a positive value for the heat of fusion but shows poor agreement for the value of the vapor pressure at the melting point. Comparison of the present measurements with the data of Hartmann and Schneider shows good agreement for the value of the vapor pressure at the melting point and a reasonable value for the heat of fusion.

The present values for calcium vapor pressures may be combined with the heat capacity data tabulated by Kelley[1] to give the following temperature dependence for the thermodynamic

---

1. K. K. Kelley, U. S. Bur. Mines Bull. No. 476 (1949).

functions for the sublimation of β-calcium:

$$\Delta F^{\circ} = 45550 - 38.76T + (0.70 \times 10^{-3})T^2 + 3.04T \log T;$$

$$\Delta H^{\circ} = 45550 - 1.32T - (0.70 \times 10^{-3})T^2;$$

$$\Delta S^{\circ} = 37.44 - 3.04 \log T - (1.40 \times 10^{-3})T.$$

Vapor pressure measurements have also been made above magnesium and above calcium-magnesium alloys. Vapor pressure measurements above triply distilled magnesium and above a 21 a/o Ca-79 a/o Mg alloy agreed within the precision of measurement. These data were combined within heat capacity data tabulated by Kelley[1] to yield the following equations for the magnesium sublimation process:

$$\Delta F^{\circ} = 35670 + 2.694T \log T + (0.75 \times 10^{-3})T^2 - (0.39 \times 10^{5})T^{-1} - 36.23T;$$

$$\Delta H^{\circ} = 35670 - 1.17T - (0.75 \times 10^{-3})T^2 - (0.78 \times 10^{5})\, T^{-1};$$

$$\Delta S^{\circ} = 35.06 - 2.694 \log T - (1.50 \times 10^{-3})T - (0.39 \times 10^{5})\, T^{-2}.$$

The vapor pressure is described in the region 600 - 900°K by the relation

$$\log P^{\circ}(\text{atm}) = 7.919 - 7796T^{-1} - 0.589 \log T - (0.16 \times 10^{-3})T + (0.85 \times 10^{4})T^{-2}.$$

Values computed from these equations are in good agreement

---

1. K. K. Kelley, U. S. Bur. Mines Bull. No. 476 (1949).

with results tabulated in various thermodynamic compilations.

Vapor pressure measurements were also made for the following alloys on the calcium-rich side of the compound: 40, 70, and 84 a/o calcium. A graphical representation of the present vapor pressure data for the calcium-magnesium system is shown in Fig. 11 and the phase diagram[1] is shown in Fig. 12. The free energy of formation of the compound, $CaMg_2$, may be expressed as

$$\Delta F^o = 2RT \ln P'/P^o$$

where P' is the vapor pressure above the region of compound plus calcium and P^o is the vapor pressure above magnesium plus compound. The vapor pressure of calcium in the alloys is negligible when compared with the vapor pressure of magnesium. This was verified by chemical analysis of the sublimate from some of the alloys.

Since no heat capacity data were available for the compound, it was assumed that $\Delta C_p = 0$ for the reaction

$$Ca\ (\alpha) + Mg(s) \rightleftharpoons CaMg_2(s).$$

The measured vapor pressures were then used to compute

$$\Delta F^o = -8.3 + (1.1 \times 10^{-3})T$$

for the free energy of formation of $CaMg_2$ in kcal/mol. The standard deviations based on a least squares fit to the

---

1. G. F. Sager and B. J. Nelson, Metals Handbook (Am. Soc. Metals, Cleveland, 1948) p 1185.

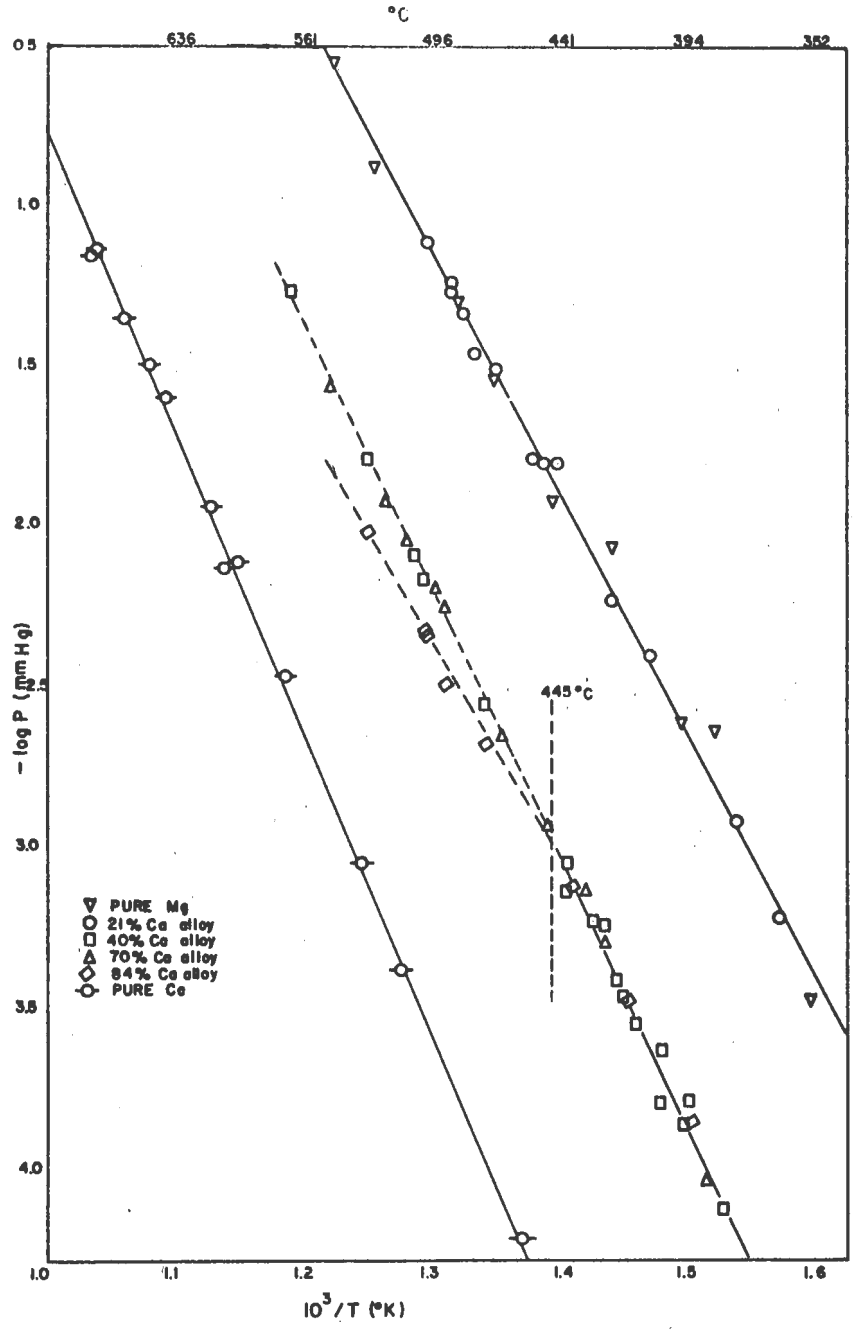

Fig. 11 - Plot of the experimentally determined vapor pressures for the calcium-magnesium system.

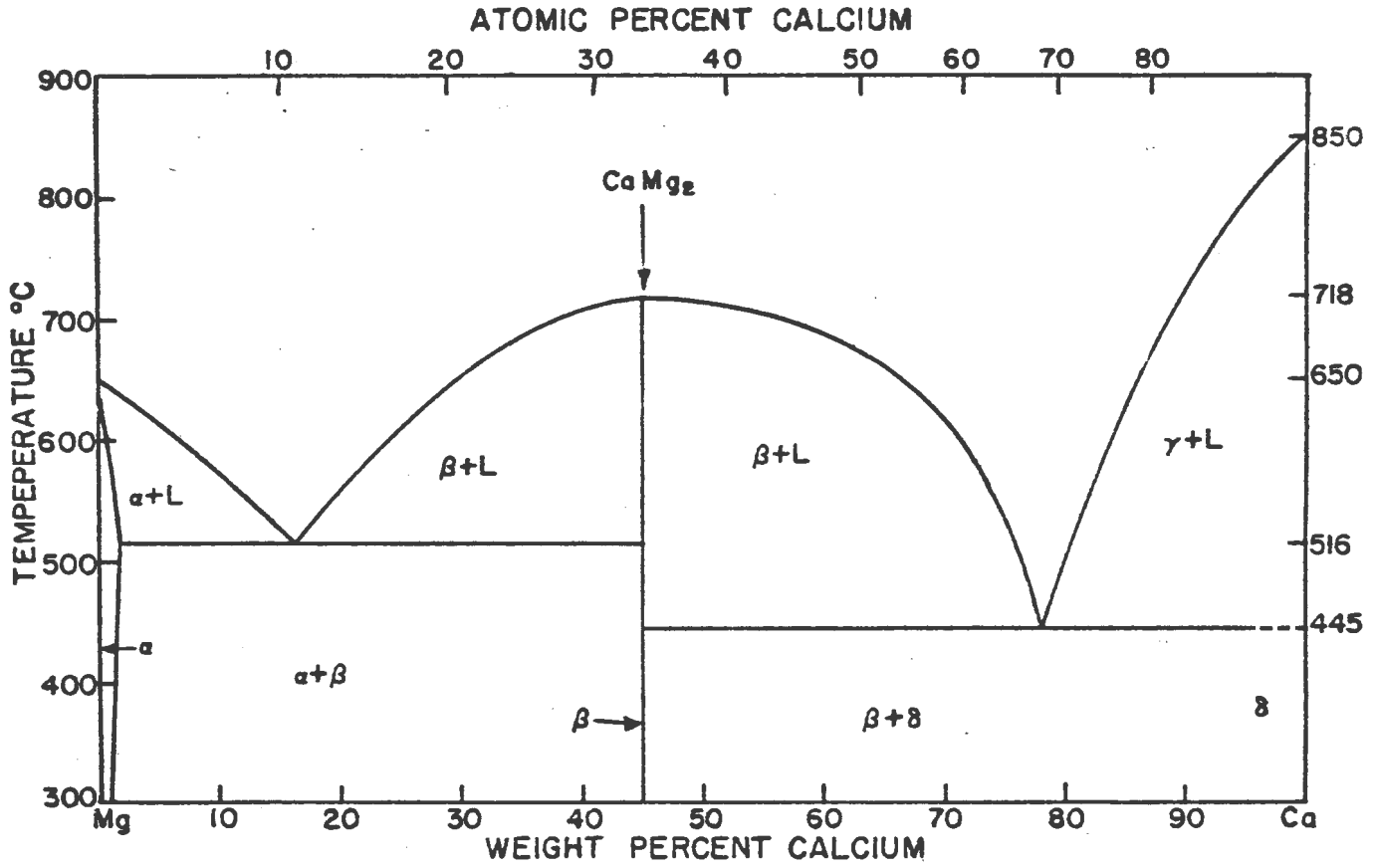

Fig. 12 - Constitution diagram of the calcium-magnesium system (after Sager and Nelson).

experimental data are ± 2.9 kcal/mol for the enthalpy and ± 4.3 eu/mol for the entropy.

8. Rare Earth Metallurgy

The major part of this material is included in ISC-976.

APPENDIX I: LIST OF REPORTS FROM THE AMES LABORATORY

1. Reports for Cooperating Laboratories

ISC-766 L. L. Knapp, M. Smutz and F. H. Spedding. Solvent Extraction Equilibria for Rare Earth Nitrate-Tributyl Phosphate Systems.

ISC-781 R. E. Bisque and C. V. Banks. Spectrophotometric Determination of Zinc and Other Metals with $\alpha, \beta, \gamma, \delta$-Tetraphenylporphine.

ISC-796 J. A. Pierret and H. A. Wilhelm. Caustic Fusion of Columbite-Tantalite Concentrates with Subsequent Separation of Niobium and Tantalum.

ISC-832 G. E. Bobeck and H. A. Wilhelm. Alloys of Aluminum, Thorium and Uranium.

ISC-834 Ames Laboratory Staff. Chemistry. Semi-Annual Summary Research Report. July-December, 1956.

ISC-835 Ames Laboratory Staff. Metallurgy. Semi-Annual Summary Research Report. July-December, 1956.

ISC-836 Ames Laboratory Staff. Engineering. Semi-Annual Summary Research Report. July-December, 1956.

ISC-837 Compiled by P. Chiotti. Hanford Slug Program. Semi-Annual Summary Research Report. July-December, 1956.

ISC-839 Donald Hunter and Glenn Murphy. Thermal Stress Analysis of a Cylinder of Semi-Plastic Material.

ISC-874 H. E. Wolfe and Glenn Murphy. Flow of an Aqueous Slurry Through a Vertical Tube.

ISC-893 H. H. Klepfer and P. Chiotti. Characteristics of the Solid State Transformations in Uranium.

ISC-899 R. W. Vest, M. Griffel and J. F. Smith. Electronic Specific Heat of Sodium Tungsten Bronze.

ISC-901 Ames Laboratory Staff. Physics. Semi-Annual Summary Research Report. January-June, 1957.

ISC-904 Ames Laboratory Staff. Engineering. Semi-Annual Summary Research Report. January-June, 1957.

ISC-905 Compiled by P. Chiotti. Hanford Slug Program. Semi-Annual Summary Research Report. January-June, 1957.

ISC-906 H. H. Klepfer, H. E. Shoemaker, J. D. Greiner, M. L. Moller and J. F. Smith. Tabulation, Bibliography, and Structure of Binary Intermetallic Compounds. III. Compounds of Copper, Silver and Gold.

ISC-908 J. E. Frandolig and R. W. Fahien. Mass Transfer in Low Velocity Gas Streams.

2. Publications

Atoji, Masao
Some New Relations Following from the Herglotz Theorem. Acta Cryst. 10, 464 (1957).

Banks, C. V., K. E. Burke, J. W. O'Laughlin and J. O. Thompson
Differential Spectrophotometric Determination of Uranium and Niobium. Anal. Chem. 29, 995-998 (1957).

Banks, C. V. and J. W. O'Laughlin
Spectrophotometric Determination of Ruthenium with 1,10-Phenanthroline. Anal. Chem. 29, 1412-1417 (1957).

Barlett, R. H., M. H. Rice and R. H. Good, Jr.
Approximations for Coulomb Wave Functions. Annals of Phys. 2, 372-383 (1957).

Burkhard, W. J. and J. D. Corbett
The Solubility of Water in Molten Mixtures of LiCl and KCl. J. Am. Chem. Soc. 79, 6361-6363 (1957).

Dahl, F. and R. E. Rundle
Polynuclear Metal Carbonyls. III. Infrared Analysis of Iron Tetracarbonyl. J. Chem. Phys. 27, 323-324 (1957).

Duke, F. R. and J. P. Cook
A Non-Visual Method for Transport Numbers in Pure Fused Salts. Iowa State Coll. J. Sci. 32, 35-37 (1957).

Duke, F. R. and N. C. Peterson
The Role of Chloride Ion in the Ferric-Stannous Reaction. A Reinterpretation Based on New Equilibrium Data. Iowa State Coll. J. Sci. 32, 89-93 (1957).

Fritz, J. S., A. J. Moye and Marlene Johnson Richard
Titration of Nitro-Aromatic Amines as Acids. Anal. Chem. 29, 1685-1688 (1957).

Fritz, J. S. and S. S. Yamamura
Differentiating Titration of Acid Mixtures in Acetone. Anal. Chem. 29, 1079-1084 (1957).

Gerstein, B. C., M. Griffel, L. D. Jennings, R. E. Miller, R. E. Skochdopole and F. H. Spedding
The Heat Capacity of Holmium from 15 to 300°K. J. Chem. Phys. 27, 394-399 (1957).

Good, R. H., Jr.
Transmission of Electrons Through Metal Surfaces. J. Appl. Phys. 28, 1405-1408 (1957).

Griffel, M., R. W. Vest and J. F. Smith
The Heat Capacity of Calcium from 1.8 to 4.2°K. J. Chem. Phys. 27, 1267-1269 (1957).

Hammer, C. L. and R. H. Good, Jr.
Wave Equation for a Massless Particle with Arbitrary Spin. Phys. Rev. 108, 882-886 (1957).

Hansen, R. S., R. E. Minturn and D. A. Hickson
Functional Group Effects in the Adsorption of Organic Compounds from Aqueous Solutions by Mercury. J. Phys. Chem. 61, 953-957 (1957).

Henry, R. M. and D. S. Martin, Jr.
Comparative Yields of (γ,2n) and (γ,pn) Processes for Fe^{54} by 70 Mev. Bremsstrahlung. Phys. Rev. 107, 772-774 (1957).

Jennings, L. D., R. M. Stanton and F. H. Spedding
The Heat Capacity of Terbium from 15 to 350°K. J. Chem. Phys. 27, 909-913 (1957).

Levine, H. B.
Equations for a Lattice Gas. II. Multicomponent Systems. J. Chem. Phys. 27, 335-342 (1957).

Moser, H. C. and A. F. Voigt
The Extraction of Mercury(II) Iodide. J. Inorg. Nucl. Chem. 4, 354-357 (1957).

Pearson, G. J., P. O. Davey and G. C. Danielson
Thermal Conductivity of Nickel and Uranium. Iowa Acad. of Sci. 64, 461-465 (1957).

Powell, J. E. and M. A. Hiller
Preparation of Carbonate-Free Bases. J. Chem. Educ. 34, 330 (1957).

Ray, A. E. and J. F. Smith
Composition Variation in the α-Phase Compound of the Vanadium-Aluminum System. Acta Cryst. 10, 604-605 (1957).

Schupp, F. D., C. B. Colvin and D. S. Martin, Jr.
Cross Section for the Ca^{40}(γ,3p3n)Cl^{34} Reaction. Phys. Rev. 107, 1058-1061 (1957).

Segel, S. L. and R. G. Barnes
Nuclear Quadrupole Moment Ratio of Re^{185} and Re^{187}. Phys. Rev. 107, 638 (1957).

Shaw, W. C., D. E. Hudson and G. C. Danielson
Electrical Properties of Boron Single Crystals. Phys. Rev. 107, 419-427 (1957).

Smith, J. F., C. E. Carlson and F. H. Spedding
The Elastic Properties of Yttrium and Eleven of the Rare Earth Elements. J. Metals, 9, 1212-1213 (1957).

Spedding, F. H.
Atomic Fuels. Metal Progress 72, No. 4, 105-111 (1957). Transactions of the 5th World Power Conference, held in Vienna, 1956, pp. 4969-4977.

Spedding, F. H., R. J. Barton and A. H. Daane
The Vapor Pressure of Thulium Metal. J. Am. Chem. Soc. 79, 5160-5163 (1957).

Spedding, F. H., A. H. Daane and K. W. Herrmann
The Electrical Resistivities and Phase Transformations of Lanthanum, Cerium, Praseodymium and Neodymium. J. Metals 9, 895-897 (1957).

Strittmater, R. C., G. J. Pearson and G. C. Danielson
Measurement of Specific Heats by a Pulse Method. Iowa Acad. of Sci. 64, 466-470 (1957).

Svec, H. J. and D. S. Gibbs
Metal-Water Reactions. V. Kinetics of the Reaction Between Magnesium and Water Vapor. J. Electrochem. Soc. 104, 434-439 (1957).

APPENDIX II: LIST OF SHIPMENTS

Destination	Item
University of Arizona Tucson, Arizona	11 gm praseodymium oxide 11 gm neodymium oxide 11 gm samarium oxide 11 gm lanthanum oxide 11 gm cerium oxide 11 gm gadolinium oxide 1 gm yttrium oxide 11 gm dysprosium oxide 11 gm holmium oxide 11 gm erbium oxide 11 gm ytterbium oxide 1 gm thulium oxide 1 gm lutetium oxide 1 gm terbium oxide
H. A. Schimming University of Wisconsin Madison, Wisconsin	50 gm cerium metal
University of California Los Alamos Scientific Laboratory Los Alamos, New Mexico	20 gm terbium metal 100 gm terbium oxide
Argonna National Laboratory Lemont, Illinois	Special discs (1 each) of cerium, neodymium and gadolinium metals
University of Denver Denver, Colorado	50 gm praseodymium metal
Purdue University Lafayette, Indiana	25 gm praseodymium oxide
Dr. James L. Kassner University of Alabama University, Alabama	2 samples of special reagent (1 gm each)
University of California Radiation Laboratory Livermore, California	1 disc each of gadolinium and erbium metals 4.82 gm dysprosium metal 3.63 gm ytterbium metal 4.31 gm holmium metal 4.21 gm terbium metal
Mrs. Mary E. White High Voltage Laboratory Cambridge 39, Massachusetts	100 mg scandium metal

Destination	Item
Bell Telephone Laboratories Murray Hill, New Jersey	2 lb dysprosium metal 2 lb neodymium metal 4.683 gm scandium metal
Dr. Joseph G. Graca Iowa State College Ames, Iowa	200 cc lutetium chloride solution 200 cc of each of the following rare earth solutions in ethylene-diaminetetraacetic acid (equivalent to 5% chloride): lanthanum gadolinium praseodymium samarium
Lincoln Laboratory Lexington, Massachusetts	100 gm yttrium oxide 100 gm samarium oxide
Physics Department Georgetown University Washington, D. C.	1 gm yttrium metal
Huffman Microanalytical Laboratory Wheatridge, Colorado	5 gm special hafnium oxide
Mr. Arnold Gahler Metals Research Laboratories Niagara Falls, New York	3 samples yttrium fluoride
Dr. Frank Benner National Research Corporation Cambridge, Massachusetts	2 samples of niobium metal 4 samples of yttrium metal
State University of Iowa Iowa City, Iowa	10 gm terbium oxide 50 gm praseodymium oxide 2 gm special N^{15} sample
Dr. Henry J. Gomberg Phoenix Memorial Laboratory University of Michigan Ann Arbor, Michigan	2 gm holmium metal 2 gm erbium metal 2 gm thulium metal 2 gm ytterbium
Union Carbide Nuclear Company Oak Ridge, Tennessee	50 gm cerium metal
Carnegie Institute of Technology Pittsburgh, Pennsylvania	4 gm cerium metal 4 gm praseodymium metal
Physikalisches Institut der Technischen Hochschule Munich, Germany	2 gm praseodymium metal 2 gm samarium metal

Destination	Item
General Electric Co. Cincinnati, Ohio	1 lb praseodymium metal 1 lb erbium metal 1 lb neodymium metal 1 lb ytterbium metal 1 lb dysprosium metal